

Inclusive Prompt Photon Production in Hadronic Final States of e^+e^- Annihilation

Edmond L. Berger¹, Xiaofeng Guo², and Jianwei Qiu²

¹*High Energy Physics Division, Argonne National Laboratory*

Argonne, Illinois 60439, USA

²*Department of Physics and Astronomy, Iowa State University*

Ames, Iowa 50011, USA

(July 27, 1995)

Abstract

We provide complete analytic expressions for the inclusive prompt photon production cross section in hadronic final states of e^+e^- annihilation reactions through one-loop order in quantum chromodynamics perturbation theory. Computed explicitly are direct photon production through first order in the electromagnetic strength α_{em} and the quark-to-photon and gluon-to-photon fragmentation contributions through first order in the strong coupling α_s . The full angular dependence of the cross sections is displayed, separated into transverse ($1 + \cos^2 \theta_\gamma$) and longitudinal ($\sin^2 \theta_\gamma$) components, where θ_γ specifies the direction of the photon with respect to the e^+e^- collision axis. We discuss extraction of fragmentation functions from e^+e^- data.

12.38.Bx, 13.65.+i, 12.38.Qk

I. INTRODUCTION

Production of an energetic photon in association with hadrons probes the short-distance dynamics of electron-positron, hadron-hadron, and lepton-hadron reactions. In addition to providing valuable tests of perturbative quantum chromodynamics (pQCD), data from electron-positron annihilation reactions permit measurements of parton-to-photon fragmentation functions.

In QCD, the quark-photon collinear singularities that arise in each order of perturbation theory, associated with the hadronic component of the photon, are subtracted and absorbed into quark-to-photon and gluon-to-photon fragmentation functions, in accord with the factorization theorem [1]. Fragmentation functions, $D(z, \mu^2)$, are inherently nonperturbative quantities whose magnitude and dependence on fractional momentum z must be measured in experiments at a reference fragmentation scale μ_0^2 . The change of $D(z, \mu^2)$ with μ^2 for large μ^2 is specified by perturbative QCD evolution equations [2]. In $e^+e^- \rightarrow \gamma X$, the fragmentation contributions play a significantly greater role than they do in hadron-hadron collisions [3]. In lowest-order, the quark-to-photon and anti-quark-to-photon fragmentation processes dominate the inclusive reaction $e^+e^- \rightarrow \gamma X$, whereas “direct” processes, such as $qg \rightarrow \gamma q$ and $q\bar{q} \rightarrow \gamma g$, dominate in $pp \rightarrow \gamma X$ and $\bar{p}p \rightarrow \gamma X$ for γ ’s that carry large values of transverse momentum [4–7]. The dominant role of fragmentation contributions makes the inclusive process $e^+e^- \rightarrow \gamma X$ a potentially ideal source of information on $D(z, \mu^2)$.

The most straightforward theoretical calculations in perturbative QCD are those for the inclusive yield of energetic photons, $E_\gamma d\sigma/d^3p_\gamma$. However, an important practical limitation of high energy investigations is that photons are observed and their cross sections are measured reliably only when the photons are relatively isolated, separated to some extent in phase space from accompanying hadrons. Since fragmentation is a process in which photons are part of quark, anti-quark, or gluon “jets”, it is evident that photon isolation reduces the contribution from fragmentation terms. In this paper, we deal with cross sections for energetic inclusive photons, and the extraction of the photon fragmentation functions $D(z, \mu^2)$.

In another paper [8], we will present a systematic and analytic treatment of cross sections for isolated photons, and show over what regions of z the functions $D(z, \mu^2)$ may be determined from data on isolated photon production in $e^+e^- \rightarrow \gamma X$. We will also point out the breakdown of factorization of the cross section for isolated photons in a particular part of phase space in $e^+e^- \rightarrow \gamma X$, and the implications of this breakdown for calculations of isolated photon production in hadronic collisions.

Our calculations of the inclusive photon yields in $e^+e^- \rightarrow \gamma X$ are carried out through one-loop order. We compute explicitly direct photon production through first order in the electromagnetic coupling strength, α_{em} , and the quark-to-photon and gluon-to-photon fragmentation contributions through first order in the strong coupling strength α_s . We display the full angular dependence of the cross sections, separated into longitudinal $\sin^2 \theta_\gamma$ and transverse components $(1 + \cos^2 \theta_\gamma)$, where θ_γ is the direction of the γ with respect to the e^+e^- collision axis. Our work goes beyond that of previous authors [9–11]. For example, the full angular dependence of the cross section was not derived before. In one recent analysis [9], the authors concentrate on events having the topology of a photon plus 1 hadronic jet; they discuss the extraction of the quark to photon fragmentation function from such data. In that approach, final state partons are treated as resolved, and the cancellation of infrared singularities is not treated explicitly. Practical aspects of confronting theoretical calculations with data from LEP are addressed in Ref. [11]. All four groups at LEP have published papers on prompt photon production [12]. In this paper, we advocate a different method of analysis of data from that used so far.

We begin in Section II with definitions of the factorized inclusive photon cross sections, and, to establish notation, we derive explicit expressions for the inclusive photon yields in lowest order ($O(\alpha_{em}^0)$, $O(\alpha_s^0)$). In Section III, we examine in turn the three 1st order contributions to the inclusive photon yield: the $O(\alpha_{em})$ process in which a photon is radiated from a final quark or antiquark line, $e^+e^- \rightarrow q\bar{q}\gamma$, and the $O(\alpha_s)$ processes in which $e^+e^- \rightarrow q\bar{q}g$, followed by fragmentation of one of the three final-state partons into a photon. The quark to photon collinear singularity in $e^+e^- \rightarrow q\bar{q}\gamma$ is absorbed into the quark-to-photon

fragmentation function. Our treatment of the $O(\alpha_s)$ contributions necessarily includes a full discussion of both real and virtual diagrams. Dimensional regularization is used to handle infrared and collinear singularities. In Section IV, we summarize our final expressions for the inclusive photon cross section $E_\gamma d\sigma_{e^+e^- \rightarrow \gamma X}/d^3\ell$, with full θ_γ dependence. Numerical results and suggestions for comparisons with e^+e^- data at LEP, SLAC/SLC, TRISTAN, and CESR/CLEO energies are also collected in Section IV. An Appendix is included in which we derive expressions for two- and three- particle phase space in n dimensions.

II. DEFINITIONS, NOTATION, AND LOWEST ORDER CONTRIBUTION

In this section we establish the notation to be used throughout the paper and present our derivation of the lowest order $O(\alpha_{em}^0 \alpha_s^0)$ contribution to the inclusive energetic photon yield in $e^+e^- \rightarrow \gamma X$.

A. General Structure of the Cross Section and Kinematics

In $e^+e^- \rightarrow cX$, as sketched in Fig. 1, the cross section for an m parton final state is

$$d\sigma^{(m)} = \frac{1}{2s} \left| \overline{M}_{e^+e^- \rightarrow c + \dots} \right|^2 dPS^{(m)} \cdot dz D_{c \rightarrow \gamma}(z), \quad (1)$$

with $c = \gamma, q, \bar{q}, g$ and $z = E_\gamma/E_c$. For inclusive photons, we integrate over all phase space, $dPS^{(m)}$, except the momentum of parton “ c ”. For isolated photons, however, the phase space, $dPS^{(m)}$, will have extra constraints due to the definition of the isolated photon events.

For the scattering amplitude, $M_{e^+e^- \rightarrow c + \dots}$, the vertex between the intermediate vector boson and the initial/final fermion pair is expressed as $ie\gamma_\mu(v_f + a_f \gamma_5)$. The absolute square of the matrix element $|\overline{M}|^2$, averaged over initial spins and summed over final spins and colors, may be expressed in terms of leptonic and hadronic tensors, $L_{\mu\nu}$ and $H^{\mu\nu}$, as

$$|\overline{M}|^2 = e^2 C \left[F^{PC}(q^2) L_{\mu\nu}^{PC} + F^{PV}(q^2) L_{\mu\nu}^{PV} \right] H^{\mu\nu}; \quad (2)$$

e denotes the electric charge, and C is the overall color factor. Since the physical observable, the energetic photon γ , does not distinguish between quarks and antiquarks, the parity violating (PV) term does not contribute. Equivalently, only the symmetric part of $H^{\mu\nu}$ contributes. Therefore,

$$|\overline{M}|^2 = e^2 C F^{PC}(q^2) L_{\mu\nu}^{PC} H^{\mu\nu} \equiv e^2 C F_q^{PC}(q^2) (H_1 + H_2). \quad (3)$$

$$H_1 = \left(-g_{\mu\nu} + \frac{q_\mu q_\nu}{q^2} \right) H^{\mu\nu} = -g_{\mu\nu} H^{\mu\nu}. \quad (4)$$

$$H_2 = -\frac{k_\mu k_\nu}{q^2} H^{\mu\nu}. \quad (5)$$

The four-momenta q^μ and k^μ are defined in terms of the four-momenta of the incident e^+ and e^- (k_1^μ and k_2^μ) as

$$q^\mu = k_1^\mu + k_2^\mu, \quad q^2 = (k_1 + k_2)^2 = s; \quad (6)$$

and

$$k^\mu = k_1^\mu - k_2^\mu, \quad k^2 = (k_1 - k_2)^2 = -s. \quad (7)$$

The normalization factor $F_q^{PC}(q^2)$ is expressed in terms of the vector (v) and axial-vector (a) couplings of the intermediate γ^* and Z^0 to the leptons and quarks. At the Z^0 pole, neglecting γ, Z^0 interference, we find

$$\frac{2}{s} F_q^{PC}(s) = (|v_e|^2 + |a_e|^2) (|v_q|^2 + |a_q|^2) \frac{1}{(s - M_Z^2)^2 + M_Z^2 \Gamma_Z^2}. \quad (8)$$

At modest energies where only the γ^* intermediate state is relevant,

$$\frac{2}{s} F_q^{PC}(s) = e_q^2 \frac{1}{s^2}; \quad (9)$$

e_q is the fractional quark charge ($e_u = 2/3; e_d = 1/3; \dots$).

In terms of functions H_1 and H_2 , defined through Eq. (3), we reexpress the cross section as

$$d\sigma^{(m)} = \sum_q \left[\frac{2}{s} F_q^{PC}(s) \right] e^2 C \frac{1}{4} (H_1 + H_2) dPS^{(m)} dz D(z). \quad (10)$$

In the sections to follow, we calculate the functions H_1 and H_2 explicitly for the lowest order and the first-order contributions to $e^+e^- \rightarrow \gamma X$. Function H_1 provides the cross section integrated over all production angles, θ_γ , of the γ . Function H_2 specifies the angular dependence or, equivalently, the transverse momentum distribution of the γ with respect to the e^+e^- collision axis.

B. Factorized Cross Section

We are interested in the inclusive cross section for production of photons in association with hadrons, $E_\gamma d\sigma_{e^+e^- \rightarrow \gamma X}^{incl} / d^3\ell$, where E_γ is the energy of the photon, and ℓ is the momentum of the photon in the e^+e^- center-of-mass system. According to the pQCD factorization theorem [1], we may express the cross section as

$$E_\gamma \frac{d\sigma_{e^+e^- \rightarrow \gamma X}^{incl}}{d^3\ell} \equiv \sum_c E_c \frac{d\hat{\sigma}_{e^+e^- \rightarrow cX}^{incl}}{d^3p_c} \otimes D_{c \rightarrow \gamma}(z). \quad (11)$$

The intermediate partons are $c = \gamma, g, q$, and \bar{q} . The hard-scattering cross section $E_c d\hat{\sigma}_{e^+e^- \rightarrow cX}^{incl} / d^3p_c$ contains no infrared or collinear divergences. The fractional momentum z is defined as $z = E_\gamma / E_c$; all intermediate partons c are assumed to be massless. The fragmentation functions $D_{c \rightarrow \gamma}(z)$ represent all long-distance physics associated with the hadronic component of the photon. They are inherently non-perturbative quantities that must be measured experimentally. Models and phenomenological parametrizations [14] for $D(z)$ have been published. In lowest-order, $D_{\gamma \rightarrow \gamma}(z) = \delta(1 - z)$. The convolution expressed in Eq. (11) is sketched in Fig. 2. The symbol \otimes in Eq. (11) is defined explicitly as follows:

$$E_c \frac{d\hat{\sigma}_{e^+e^- \rightarrow cX}^{incl}}{d^3p_c} \otimes D_{c \rightarrow \gamma}(z) \equiv \int_{z_{\min}}^1 \frac{dz}{z^2} \left[E_c \frac{d\hat{\sigma}_{e^+e^- \rightarrow cX}^{incl} \left(E_c = \frac{E_\gamma}{z} \right)}{d^3p_c} \right] D_{c \rightarrow \gamma}(z). \quad (12)$$

Since z_{\min} occurs when p_c has its maximum value, $p_c^{\max} = \sqrt{s}/2$, the lower limit of integration $z_{\min} = x_\gamma = 2E_\gamma/\sqrt{s}$; \sqrt{s} is the center of mass energy of the e^+e^- annihilation.

C. Derivation of the Lowest Order Contribution

In this section we present an explicit derivation of the lowest order contribution to the inclusive photon yield in $e^+e^- \rightarrow \gamma$, sketched in Fig. 3. The differential inclusive cross section $d\sigma_{e^+e^- \rightarrow \gamma X}$ is expressed as a product of the lowest order partonic cross section $d\hat{\sigma}_{e^+e^- \rightarrow q\bar{q}}^{(o)}$ and the $q \rightarrow \gamma$ fragmentation function, $D_{q \rightarrow \gamma}(z)$.

$$d\sigma_{e^+e^- \rightarrow \gamma X} = \sum_q d\hat{\sigma}_{e^+e^- \rightarrow q(p_q)\bar{q}}^{(o)} dz D_{p_q \rightarrow \gamma}(z) + (q \rightarrow \bar{q}). \quad (13)$$

In Eq. (13), p_q is the four-vector momentum of the quark q , and $z = \ell/p_q$. The partonic cross section is written, in turn, in terms of the invariant matrix element and differential phase space factor.

$$\begin{aligned} d\hat{\sigma}_{e^+e^- \rightarrow p_q p_{\bar{q}}}^{(o)} &= \frac{1}{2s} \left| \overline{M}_{e^+e^- \rightarrow p_q p_{\bar{q}}} \right|^2 dPS^{(2)} \\ &= \left[\frac{2}{s} F_q^{PC}(s) \right] e^2 N_c \frac{1}{4} (H_1 + H_2) dPS^{(2)}, \end{aligned} \quad (14)$$

where $N_c = 3$ is the number of colors carried by the quarks, and Eq. (3) was used.

The symmetric part of the hadronic tensor $H^{\mu\nu}$, used to define functions H_1 and H_2 , is particularly simple:

$$H^{\mu\nu} = 4(e\mu^\epsilon)^2 \left[p_q^\mu p_{\bar{q}}^\nu + p_{\bar{q}}^\mu p_q^\nu - g^{\mu\nu} p_q \cdot p_{\bar{q}} \right]. \quad (15)$$

The factor μ^ϵ in Eq. (15) accommodates the fact that we are working in n dimensions. The dimensional scale μ will be specified further below. The functions H_1 and H_2 , defined in Section II A, become

$$H_1 = 4(e\mu^\epsilon)^2 s (1 - \epsilon); \quad (16a)$$

$$H_2 = -2(e\mu^\epsilon)^2 s (1 - \cos^2 \theta). \quad (16b)$$

In Eq. (15), ϵ is defined through the number of space dimensions $n = 4 - 2\epsilon$, with $\epsilon \rightarrow 0$ at the end of the calculation. In the center of mass frame of the collision, θ is the angle of \vec{p}_q with respect to the direction defined by the incident e^+ . Combining H_1 and H_2 , we obtain

$$\frac{1}{4} (H_1 + H_2) = \frac{1}{2} (e\mu^\epsilon)^2 s \left[(1 + \cos^2 \theta) - 2\epsilon \right]. \quad (17)$$

Combining Eqs. (17) and the expression for two-particle phase space in n -dimensions, Eq. (A4) of the Appendix, we find that the lowest order partonic cross section, Eq. (14), is

$$E_q \frac{d\hat{\sigma}_{e^+e^- \rightarrow qX}^{(0)}}{d^3 p_q} = \left[\frac{2}{s} F_q^{PC}(s) \right] \alpha_{em}^2 N_c \left(\frac{4\pi\mu^2}{(s/4)\sin^2\theta} \right)^\epsilon \frac{1}{\Gamma(1-\epsilon)} \left[(1 + \cos^2 \theta) - 2\epsilon \right] \frac{\delta(x_q - 1)}{x_q}, \quad (18)$$

with $x_q = 2E_q/\sqrt{s}$. At this order, the cross section is manifestly finite in the limit $\epsilon \rightarrow 0$, and we may set $\epsilon = 0$ directly in Eq. (18). Nevertheless, Eq. (18) expressed in n dimensions is valuable for later comparison with the higher order cross section.

Noting that $\ell = zp_q$ implies $d^3 p_q/E_q = (1/z^2) d^3 \ell/E_\gamma$, we obtain the lowest order inclusive cross section

$$\begin{aligned} E_\gamma \frac{d\sigma_{e^+e^- \rightarrow \gamma X}^{incl}}{d^3 \ell} &= 2 \sum_q \int^1 \frac{dz}{z^2} \left[E_q \frac{d\hat{\sigma}_{e^+e^- \rightarrow qX}^{(0)}}{d^3 p_q} \left(x_q = \frac{x_\gamma}{z} \right) \right] D_{q \rightarrow \gamma}(z, \mu_F) \\ &= 2 \sum_q \left[\frac{2}{s} F_q^{PC}(s) \right] \alpha_{em}^2 N_c (1 + \cos^2 \theta_\gamma) \frac{1}{x_\gamma} D_{q \rightarrow \gamma}(x_\gamma, \mu_F). \end{aligned} \quad (19)$$

The angles θ_γ and θ are identical since we take all products of the fragmentation to be collinear. The overall factor of 2 in Eq. (19) accounts for the \bar{q} contribution. In Eq. (19) we have introduced a fragmentation scale μ_F in the specification of the fragmentation function.

III. FIRST ORDER CONTRIBUTIONS

There are three distinct contributions to $e^+e^- \rightarrow \gamma X$ in first order perturbation theory:

$$e^+e^- \rightarrow \gamma, \quad O(\alpha_{em}) \quad (20a)$$

$$e^+e^- \rightarrow q \text{ (or } \bar{q} \text{)} \rightarrow \gamma, \quad O(\alpha_s) \quad (20b)$$

and

$$e^+e^- \rightarrow g \rightarrow \gamma. \quad O(\alpha_s) \quad (20c)$$

In Eqs. (20b) and (20c), we have in mind contributions from quark and gluon fragmentation to photons in the three-parton final state process $e^+e^- \rightarrow q\bar{q}g$. The first contribution, Eq. (20a), arises from $e^+e^- \rightarrow q\bar{q}\gamma$ where the γ is not collinear with either \bar{q} or q .

In this section we derive and present the explicit contributions to the inclusive yield $E_\gamma d\sigma_{e^+e^- \rightarrow \gamma X}^{incl}/d^3\ell$ from each of the three processes in Eq. (20). Following the pQCD factorization theorem, and Eq. (11), we must calculate the short-distance hard-scattering cross sections, $E_c d\hat{\sigma}_{e^+e^- \rightarrow cX}^{incl}/d^3p_c$ for $c = \gamma, g, q$ and \bar{q} .

The Feynman graphs for $e^+e^- \rightarrow \gamma q\bar{q}$ are sketched in Fig. 4. Owing to the quark-photon collinear divergence, the cross section associated with these graphs is formally divergent. We denote this divergent first order cross-section $\sigma_{e^+e^- \rightarrow \gamma X}^{(1)}$, a short-hand notation for $E d\sigma/d^3\ell$. To derive the corresponding short-distance hard-scattering cross section, $\hat{\sigma}_{e^+e^- \rightarrow \gamma X}^{(1)}$, we apply the factorized form, Eq. (11), perturbatively,

$$\begin{aligned} \sigma_{e^+e^- \rightarrow \gamma X}^{(1)} &= \hat{\sigma}_{e^+e^- \rightarrow \gamma X}^{(1)} \otimes D_{\gamma \rightarrow \gamma}^{(0)}(z) \\ &+ \hat{\sigma}_{e^+e^- \rightarrow q X}^{(0)} \otimes D_{q \rightarrow \gamma}^{(1)}(z) \\ &+ (q \rightarrow \bar{q}). \end{aligned} \quad (21)$$

The convolution represented by \otimes is defined in Eq. (12). The superscripts (0) and (1) on the hard-scattering cross sections $\hat{\sigma}$ and fragmentation functions D refer to lowest-order and first order, respectively. The collinear divergence resides in the first order fragmentation function $D_{q \rightarrow \gamma}^{(1)}(z)$. The hard-scattering cross sections $\hat{\sigma}^{(1)}$ and $\hat{\sigma}^{(0)}$ are finite. The expression for $\hat{\sigma}^{(0)}$ was derived in Section II C. In Section A we present our derivation of $\hat{\sigma}_{e^+e^- \rightarrow \gamma X}^{(1)}$:

$$\hat{\sigma}_{e^+e^- \rightarrow \gamma X}^{(1)} = \sigma_{e^+e^- \rightarrow \gamma X}^{(1)} - \hat{\sigma}_{e^+e^- \rightarrow q X}^{(0)} \otimes D_{q \rightarrow \gamma}^{(1)}(z) - (q \rightarrow \bar{q}). \quad (22)$$

The two Feynman graphs that provide the cross section for $e^+e^- \rightarrow g \rightarrow \gamma$ in $O(\alpha_s)$ are shown in Fig. 5. In this case, the final gluon is effectively “observed” through the fragmentation $g \rightarrow \gamma$; there are no virtual gluon exchange diagrams. The finite hard-scattering cross section $\hat{\sigma}_{e^+e^- \rightarrow g X}^{(1)}$ is derived from the difference

$$\hat{\sigma}_{e^+e^- \rightarrow g X}^{(1)} = \sigma_{e^+e^- \rightarrow g X}^{(1)} - \sum_{q'=q}^{\bar{q}} \hat{\sigma}_{e^+e^- \rightarrow q' X}^{(0)} \otimes D_{q' \rightarrow g}^{(1)}. \quad (23)$$

In Eq. (23), the divergent cross section $\sigma_{e^+e^- \rightarrow gX}^{(1)}$ is evaluated from the Feynman graphs shown in Fig. 5, and the quark-to-gluon collinear divergences are embedded in the first-order fragmentation function $D_{q' \rightarrow g}^{(1)}$. Our derivation of $\hat{\sigma}_{e^+e^- \rightarrow gX}^{(1)}$ is presented in Section B.

The Feynman graphs in $O(\alpha_s)$ that contribute to $e^+e^- \rightarrow q \rightarrow \gamma$ (Eq. (20b)) are sketched in Fig. 6. Only a final state photon from quark fragmentation is observed. The complete $O(\alpha_s)$ result includes both real gluon emission and virtual gluon exchange graphs, as shown in Fig. 6. Although infrared divergences associated with soft gluons cancel between the real and virtual graphs, the cross section $\sigma_{e^+e^- \rightarrow qX}^{(1)}$ obtained from the Feynman graphs is still divergent due to collinear singularities when the real gluon is emitted along the direction of its parent quark or antiquark. To obtain the corresponding hard-scattering cross section $\hat{\sigma}_{e^+e^- \rightarrow qX}^{(1)}$, we apply the factorized form, Eq. (11), perturbatively, to the production of a quark instead of the photon,

$$\sigma_{e^+e^- \rightarrow qX}^{(1)} = \sum_{q'=q}^{\bar{q}} \hat{\sigma}_{e^+e^- \rightarrow q'}^{(0)} \otimes D_{q' \rightarrow q}^{(1)} + \hat{\sigma}_{e^+e^- \rightarrow qX}^{(1)} \otimes D_{q \rightarrow q}^{(0)}, \quad (24)$$

with the collinear $q' \rightarrow q$ singularities in $O(\alpha_s)$ included in $D_{q' \rightarrow q}^{(1)}$. Note that $D_{q \rightarrow q}^{(0)}(z) = \delta(1-z)$. Correspondingly, the finite hard-scattering cross section $\hat{\sigma}_{e^+e^- \rightarrow qX}^{(1)}$ is

$$\hat{\sigma}_{e^+e^- \rightarrow qX}^{(1)} = \sigma_{e^+e^- \rightarrow qX}^{(1)} - \hat{\sigma}_{e^+e^- \rightarrow q}^{(0)} \otimes D_{q \rightarrow q}^{(1)}. \quad (25)$$

In Section C we present a detailed derivation of $\hat{\sigma}_{e^+e^- \rightarrow qX}^{(1)}$.

Before turning to our explicit derivations, we conclude this discussion with a presentation of the factorized formula for the two-loop short-distance hard-scattering cross sections. The two-loop direct contribution to $e^+e^- \rightarrow \gamma X$ is of $O(\alpha_{em}\alpha_s)$ and can be derived as follows. We first apply the factorized form, Eq. (11), perturbatively, at two-loop level and sum over $c = \gamma, g, q$ and \bar{q} ,

$$\begin{aligned} \sigma_{e^+e^- \rightarrow \gamma X}^{(2)} &= \hat{\sigma}_{e^+e^- \rightarrow \gamma X}^{(2)} \otimes D_{\gamma \rightarrow \gamma}^{(0)}(z) + \hat{\sigma}_{e^+e^- \rightarrow \gamma X}^{(1)} \otimes D_{\gamma \rightarrow \gamma}^{(1)}(z) \\ &\quad + \hat{\sigma}_{e^+e^- \rightarrow g X}^{(1)} \otimes D_{g \rightarrow \gamma}^{(1)}(z) + \hat{\sigma}_{e^+e^- \rightarrow g X}^{(0)} \otimes D_{g \rightarrow \gamma}^{(2)}(z) \\ &\quad + \hat{\sigma}_{e^+e^- \rightarrow q X}^{(1)} \otimes D_{q \rightarrow \gamma}^{(1)}(z) + \hat{\sigma}_{e^+e^- \rightarrow q X}^{(0)} \otimes D_{q \rightarrow \gamma}^{(2)}(z) \\ &\quad + (q \rightarrow \bar{q}). \end{aligned} \quad (26)$$

All first-order contributions, $\hat{\sigma}^{(1)}$, in Eq. (26) are given in Eqs. (22), (23) and (25), and they are calculated in this paper. Since the first order fragmentation functions $D_{\gamma \rightarrow \gamma}^{(1)}(z)$ and $D_{g \rightarrow \gamma}^{(1)}(z)$ vanish, and the zeroth order hard-scattering cross section $\hat{\sigma}_{e^+e^- \rightarrow gX}^{(0)}$ vanishes, we derive the two-loop hard-scattering cross sections $\hat{\sigma}_{e^+e^- \rightarrow \gamma X}^{(2)}$ as:

$$\begin{aligned} \hat{\sigma}_{e^+e^- \rightarrow \gamma X}^{(2)} &= \sigma_{e^+e^- \rightarrow \gamma X}^{(2)} \\ &- \hat{\sigma}_{e^+e^- \rightarrow qX}^{(1)} \otimes D_{q \rightarrow \gamma}^{(1)}(z) - \hat{\sigma}_{e^+e^- \rightarrow qX}^{(0)} \otimes D_{q \rightarrow \gamma}^{(2)}(z) \\ &- (q \rightarrow \bar{q}). \end{aligned} \quad (27)$$

To complete the calculation of $\hat{\sigma}_{e^+e^- \rightarrow \gamma X}^{(2)}$, it is necessary to calculate the two-loop parton-level cross section $\sigma_{e^+e^- \rightarrow \gamma X}^{(2)}$ and the two-loop quark-to-photon fragmentation function $D_{q \rightarrow \gamma}^{(2)}(z)$ in n -dimensions (implicitly, we use dimensional regularization), in addition to all the zeroth and first order contributions calculated in this paper. The two-loop parton level cross section $\sigma_{e^+e^- \rightarrow \gamma X}^{(2)}$ is formally divergent. As is true of the calculation of $\hat{\sigma}_{e^+e^- \rightarrow qX}^{(1)}$ in Section III C, all infrared divergences associated with soft gluons cancel among the real emission and virtual exchange diagrams. All collinear divergences that appear when final-state quarks and/or gluons are parallel to the observed photon are cancelled by the subtraction terms given in Eq. (27). Consequently, the two-loop hard-scattering cross section $\hat{\sigma}_{e^+e^- \rightarrow \gamma X}^{(2)}$ is finite if the pQCD factorization theorem holds.

As shown in Section IV, the leading order short-distance direct production contribution $\hat{\sigma}_{e^+e^- \rightarrow \gamma X}^{(1)}$ is much smaller than the leading order fragmentation contribution $\hat{\sigma}_{e^+e^- \rightarrow qX}^{(0)} \otimes D_{q \rightarrow \gamma}^{(1)}(z) + (q \leftrightarrow \bar{q})$. We expect that the next-to-leading order direct contribution $\hat{\sigma}_{e^+e^- \rightarrow \gamma X}^{(2)}$ will be much smaller than the next-to-leading order fragmentation contributions $\hat{\sigma}_{e^+e^- \rightarrow cX}^{(1)} \otimes D_{c \rightarrow \gamma}^{(1)}(z)$ with $c = g, q$ and \bar{q} , which are completely derived in this paper. We will not calculate the two-loop contributions in this paper because we believe their contributions to the overall cross section are much too small in comparison with those presented here.

A. Derivation of $\hat{\sigma}_{e^+e^-\rightarrow\gamma X}^{(1)}$

In this section we present an explicit derivation of the finite hard-scattering cross section $\hat{\sigma}_{e^+e^-\rightarrow\gamma X}^{(1)}$ in $O(\alpha_{em})$. We begin by computing the functions H_1 and H_2 , defined in Section II A, Eqs. (4) and (5). These will then be integrated over phase space to yield the cross section $E_\gamma d\sigma_{e^+e^-\rightarrow\gamma X}^{(1)}/d^3\ell$:

$$d\sigma_{e^+e^-\rightarrow\gamma X}^{(1)} = \sum_q \left[\frac{2}{s} F_q^{PC}(s) \right] e^2 N_c \frac{1}{4} (H_1 + H_2) dPS^{(3)}, \quad (28)$$

where three-particle phase space in n -dimensions is given in Eq. (A29) of the Appendix.

Sketched in Fig. 7 is the hadronic tensor $H_{\mu\nu}$ obtained from the two diagrams of Fig. 4. Performing traces to sum over final spins, we may write the four contributions as

$$\begin{aligned} H_{\mu\nu}^{(a)} &= 2(1-\epsilon) Tr [\gamma_\mu \gamma \cdot \ell \gamma_\nu \gamma \cdot p_2] \frac{1}{2p_1 \cdot \ell}; \\ H_{\mu\nu}^{(b)} &= 2(1-\epsilon) Tr [\gamma_\mu \gamma \cdot p_1 \gamma_\nu \gamma \cdot \ell] \frac{1}{2p_2 \cdot \ell}; \\ H_{\mu\nu}^{(c)} &= -2 Tr [\gamma_\mu \gamma \cdot p_1 \gamma \cdot p_2 \gamma_\nu \gamma \cdot (p_1 + \ell) \gamma \cdot (p_2 + \ell)] \frac{1}{2p_1 \cdot \ell} \frac{1}{2p_2 \cdot \ell} \\ &\quad + 2\epsilon Tr [\gamma_\mu \gamma \cdot p_1 \gamma \cdot \ell \gamma_\nu \gamma \cdot p_2 \gamma \cdot \ell] \frac{1}{2p_1 \cdot \ell} \frac{1}{2p_2 \cdot \ell}; \\ H_{\mu\nu}^{(d)} &= -2 Tr [\gamma_\mu \gamma \cdot (p_1 + \ell) \gamma \cdot (p_2 + \ell) \gamma_\nu \gamma \cdot p_1 \gamma \cdot p_2] \frac{1}{2p_1 \cdot \ell} \frac{1}{2p_2 \cdot \ell} \\ &\quad + 2\epsilon Tr [\gamma_\mu \gamma \cdot \ell \gamma \cdot p_1 \gamma_\nu \gamma \cdot \ell \gamma \cdot p_2] \frac{1}{2p_1 \cdot \ell} \frac{1}{2p_2 \cdot \ell}. \end{aligned} \quad (29)$$

To obviate multiple repetition of a common factor, we temporarily omit the overall coupling factor $e_q^2 (e\mu^\epsilon)^4$ that appears in $H_{\mu\nu}$. Function $H_1 = -g_{\mu\nu} H^{\mu\nu} = -g_{\mu\nu} \sum_{i=a}^d H^{(i)\mu\nu}$. We obtain

$$H_1 = 8(1-\epsilon) \left\{ (1-\epsilon) \left[\frac{y_{1\ell}}{y_{2\ell}} + \frac{y_{2\ell}}{y_{1\ell}} \right] + \frac{2y_{12}}{y_{1\ell} y_{2\ell}} - 2\epsilon \right\}. \quad (30)$$

The dimensionless quantities $y_{1\ell}$, $y_{2\ell}$, and y_{12} are defined by

$$\begin{aligned} y_{i\ell} &= \frac{2p_i \cdot \ell}{q^2} \quad (i = 1, 2); \\ y_{12} &= \frac{2p_1 \cdot p_2}{q^2}. \end{aligned} \quad (31)$$

We remark that $y_{12} + y_{1\ell} + y_{2\ell} = 1$. In evaluating $H_2 = -(k_\mu k_\nu / q^2) H^{\mu\nu}$, we also make use of dimensionless quantities y_{1k} , y_{2k} , and $y_{k\ell}$:

$$\begin{aligned} y_{ik} &= \frac{2p_i \cdot k}{q^2} \quad (i = 1, 2); \\ y_{k\ell} &= \frac{2k \cdot \ell}{q^2}. \end{aligned} \quad (32)$$

Because $k \cdot q = 0$,

$$y_{1k} + y_{2k} + y_{k\ell} = 0. \quad (33)$$

After some algebra we find

$$\begin{aligned} H_2 &= -4 \left\{ (1 - \epsilon) \left[\frac{y_{1\ell}}{y_{2\ell}} + \frac{y_{2\ell}}{y_{1\ell}} \right] + \frac{2y_{12}}{y_{1\ell} y_{2\ell}} - 2\epsilon \right\} \\ &\quad + \frac{4}{y_{1\ell} y_{2\ell}} \left\{ y_{1k}^2 + y_{2k}^2 \right\} - \frac{4\epsilon}{y_{1\ell} y_{2\ell}} \left\{ y_{k\ell}^2 \right\}. \end{aligned} \quad (34)$$

Our next task is to integrate H_1 and H_2 over three-body phase space in $n = 4 - 2\epsilon$ dimensions. Since the momentum of the photon (ℓ) is an observable, and the momentum of either the quark (p_1) or antiquark (p_2) can be fixed by the overall momentum conservation δ -function in the three-body phase space, we need to integrate over only p_1 or p_2 . In the following discussion, we let p_2 be fixed by the δ -function, and we integrate over p_1 . In the overall center of mass frame, as sketched in Fig. 8, we take angle θ_γ to be the polar angle of the γ with respect to the e^+e^- collision axis and angle $\theta_{1\gamma}$ to be the angle between the γ 's momentum ℓ and the quark momentum p_1 . The angle θ_x is the n -dimensional generalization of the three-dimensional azimuthal angle ϕ , defined through p_1 as

$$d\Omega_{n-2}(p_1) \equiv d\theta_{1\gamma} \sin^{n-3} \theta_{1\gamma} d\theta_x \sin^{n-4} \theta_x d\Omega_{n-4}(p_1). \quad (35)$$

Having chosen the frame, we may reexpress the y variables in terms of observables and integration angles as follows:

$$\begin{aligned} y_{k\ell} &= -x_\gamma \cos \theta_\gamma, \\ y_{1k} &= - \left[\frac{y_{2\ell} y_{12} - y_{1\ell}}{x_\gamma} \right] \cos \theta_\gamma - \left[\frac{2\sqrt{y_{12} y_{1\ell} y_{2\ell}}}{x_\gamma} \right] \sin \theta_\gamma \cos \theta_x; \\ y_{2k} &= - \left[\frac{y_{1\ell} y_{12} - y_{2\ell}}{x_\gamma} \right] \cos \theta_\gamma + \left[\frac{2\sqrt{y_{12} y_{1\ell} y_{2\ell}}}{x_\gamma} \right] \sin \theta_\gamma \cos \theta_x; \end{aligned} \quad (36)$$

where $x_\gamma = 2E_\gamma/\sqrt{s} (= y_{1\ell} + y_{2\ell})$. In deriving y_{1k} and y_{2k} , we use the following identities

$$\begin{aligned}\cos \theta_{1\gamma} &= \frac{y_{2\ell}y_{12} - y_{1\ell}}{x_1 x_\gamma} ; \\ \sin \theta_{1\gamma} &= \frac{2\sqrt{y_{12}y_{1\ell}y_{2\ell}}}{x_1 x_\gamma} ,\end{aligned}\tag{37}$$

where $x_1 = 2E_1/\sqrt{s}$.

In the integration of H_2 over phase space, the integral over $d \cos \theta_x$ is done from $\cos \theta_x = -1$ to $+1$. The expression for the three-body phase space, Eq. (A23), is an even function of $\cos \theta_x$. Correspondingly, terms in H_2 that are odd functions of $\cos \theta_x$ do not survive. Because H_2 depends only on the square of the y_{1k} and y_{2k} , after eliminating all terms linear in $\cos \theta_x$, we find that the only θ_x dependence in H_2 is $\cos^2 \theta_x$. We can integrate over θ_x independent of other variables, or we can effectively replace the $\cos^2 \theta_x$ terms in H_2 by the average of $\cos^2 \theta_x$ in n -dimensions and eliminate the θ_x dependence in H_2 completely.

Given the average of $\cos^2 \theta_x$ in n -dimensions, Eq. (A26), we obtain, effectively,

$$\begin{aligned}y_{k\ell}^2 &= x_\gamma^2 \cos^2 \theta_\gamma ; \\ y_{1k}^2 &= \left[\frac{y_{2\ell}y_{12} - y_{1\ell}}{x_\gamma} \right]^2 \cos^2 \theta_\gamma + \left(\frac{1}{1-\epsilon} \right) \left[\frac{2(y_{12}y_{1\ell}y_{2\ell})}{x_\gamma^2} \right] \sin^2 \theta_\gamma ; \\ y_{2k}^2 &= \left[\frac{y_{1\ell}y_{12} - y_{2\ell}}{x_\gamma} \right]^2 \cos^2 \theta_\gamma + \left(\frac{1}{1-\epsilon} \right) \left[\frac{2(y_{12}y_{1\ell}y_{2\ell})}{x_\gamma^2} \right] \sin^2 \theta_\gamma ;\end{aligned}\tag{38}$$

where the factor $1/(1-\epsilon)$ is from the average of $\cos^2 \theta_x$. Substituting the above expressions into Eq. (34), and combining with H_1 in Eq. (30), we obtain,

$$\begin{aligned}\frac{1}{4} (H_1 + H_2^{eff}) &= (1 + \cos^2 \theta_\gamma - 2\epsilon) \left[(1-\epsilon) \left(\frac{y_{1\ell}}{y_{2\ell}} + \frac{y_{2\ell}}{y_{1\ell}} \right) + 2 \left(\frac{y_{12}}{y_{1\ell}y_{2\ell}} - \epsilon \right) \right] \\ &\quad + (1 - 3 \cos^2 \theta_\gamma) \left[\frac{4y_{12}}{x_\gamma^2} \right] \\ &\quad + \left(\frac{\epsilon}{1-\epsilon} \right) (1 - \cos^2 \theta_\gamma) \left[\frac{4y_{12}}{x_\gamma^2} \right] ,\end{aligned}\tag{39}$$

where the superscript “ eff ” indicates that we have replaced $\cos^2 \theta_x$ by its average in n -dimensions. The two δ -functions in the three-particle phase space, $dPS^{(3)}$, provide the following identities

$$\begin{aligned}
y_{12} &= 1 - x_\gamma ; \\
y_{2\ell} &= x_\gamma - y_{1\ell} .
\end{aligned} \tag{40}$$

Introducing $\hat{y}_{1\ell} = y_{1\ell}/x_\gamma$, and substituting these identities into Eq. (39), we derive

$$\begin{aligned}
\frac{1}{4} (H_1 + H_2^{eff}) &= (1 + \cos^2 \theta_\gamma - 2\epsilon) \left[\frac{1 + (1 - x_\gamma)^2}{x_\gamma^2} \right] \left(\frac{1}{\hat{y}_{1\ell}} + \frac{1}{1 - \hat{y}_{1\ell}} \right) \\
&+ (1 + \cos^2 \theta_\gamma - 2\epsilon) \left[-2 - \epsilon \left(\frac{1}{\hat{y}_{1\ell}} + \frac{1}{1 - \hat{y}_{1\ell}} \right) \right] \\
&+ (1 - 3 \cos^2 \theta_\gamma) \left[\frac{4(1 - x_\gamma)}{x_\gamma^2} \right] \\
&+ \left(\frac{\epsilon}{1 - \epsilon} \right) (1 - \cos^2 \theta_\gamma) \left[\frac{4(1 - x_\gamma)}{x_\gamma^2} \right] .
\end{aligned} \tag{41}$$

The last term vanishes as $\epsilon \rightarrow 0$.

Combining Eqs. (28) and (41), and integrating over $d\hat{y}_{1\ell}$, we can derive the partonic cross section $d\sigma_{e^+e^- \rightarrow \gamma X}^{(1)}$. The limits of the $d\hat{y}_{1\ell}$ integration are from 0 to 1. The integrals over $d\hat{y}_{1\ell}$ for $(H_1 + H_2^{eff})/4$ may be expressed in terms of

$$I_{n,m} \equiv \int_0^1 d\hat{y}_{1\ell} \hat{y}_{1\ell}^{n-\epsilon} (1 - \hat{y}_{1\ell})^{m-\epsilon}. \tag{42}$$

Examining Eq. (41), we need only $I_{0,0}$ and $I_{-1,0}$ ($= I_{0,-1}$):

$$I_{0,0} = B(1 - \epsilon, 1 - \epsilon) = \frac{(\Gamma(1 - \epsilon))^2}{\Gamma(2 - 2\epsilon)}; \tag{43}$$

$$I_{-1,0} = B(-\epsilon, 1 - \epsilon) = \left(\frac{1}{-\epsilon} \right) \frac{(\Gamma(1 - \epsilon))^2}{\Gamma(1 - 2\epsilon)}. \tag{44}$$

For small ϵ , $I_{0,0} = 1 + O(\epsilon)$, and $I_{-1,0} = -\frac{1}{\epsilon} + O(\epsilon)$.

After performing the integration over $d\hat{y}_{1\ell}$, we expand the right-hand side of Eq. (28) in a power series in ϵ , keeping only the singular term proportional to $(1/\epsilon)$ and the terms independent of ϵ . (Terms of $O(\epsilon^m)$, $m \geq 1$, vanish in the physical limit of four dimensions ($n = 4 - 2\epsilon$)). We obtain

$$\begin{aligned}
E_\gamma \frac{d\sigma_{e^+e^- \rightarrow \gamma X}^{(1)}}{d^3\ell} = & 2 \sum_q \left[\frac{2}{s} F_q^{PC}(s) \right] \left[\alpha_{em}^2 N_c \left(\frac{4\pi\mu^2}{(s/4)\sin^2\theta_\gamma} \right)^\epsilon \frac{1}{\Gamma(1-\epsilon)} \right] (1 + \cos^2\theta_\gamma - 2\epsilon) \\
& \times \frac{1}{x_\gamma} \left\{ e_q^2 \frac{\alpha_{em}}{2\pi} \left[\frac{1 + (1 - x_\gamma)^2}{x_\gamma} \right] \right\} \left(-\frac{1}{\epsilon} \right) \\
& + 2 \sum_q \left[\frac{2}{s} F_q^{PC}(s) \right] \left[\alpha_{em}^2 N_c \frac{1}{x_\gamma} \right] e_q^2 \left(\frac{\alpha_{em}}{2\pi} \right) \\
& \times \left\{ (1 + \cos^2\theta_\gamma) \left[\frac{1 + (1 - x_\gamma)^2}{x_\gamma} \right] [\ell n(s/\mu_{\overline{MS}}^2) + \ell n(x_\gamma^2(1 - x_\gamma))] \right. \\
& \left. + (1 - 3\cos^2\theta_\gamma) \left[\frac{2(1 - x_\gamma)}{x_\gamma} \right] \right\}. \tag{45}
\end{aligned}$$

In deriving Eq. (45), we included the overall factor for coupling constants, $e_q^2 (e\mu^\epsilon)^4$; and used the expansion $\Gamma(1 - \epsilon) \simeq 1 + \epsilon\gamma_E$, where γ_E is Euler's constant, and the usual modified minimal subtraction scale

$$\mu_{\overline{MS}}^2 \equiv \mu^2 4\pi e^{-\gamma_E}. \tag{46}$$

The $(1/\epsilon)$ singularity in Eq. (45) represents the quark-photon collinear singularity. This singular term is expected to be cancelled by subtraction terms defined in Eq. (22). By evaluating the diagram sketched in Fig. 9, we obtain the one-loop quark-to-photon fragmentation function

$$D_{q \rightarrow \gamma}^{(1)}(z) = D_{\bar{q} \rightarrow \gamma}^{(1)}(z) = e_q^2 \frac{\alpha_{em}}{2\pi} \left[\frac{1 + (1 - z)^2}{z} \right] \left(\frac{1}{-\epsilon} \right), \tag{47}$$

where we keep only the $1/\epsilon$ pole term because we work in the \overline{MS} factorization scheme. Using the fact that $D_{\bar{q} \rightarrow \gamma}^{(1)}(z) = D_{q \rightarrow \gamma}^{(1)}(z)$, and comparing Eq. (45) with Eqs. (18) and (47), we observe that the divergent first term in Eq. (45) is cancelled exactly by the subtraction terms defined in Eq. (22), in accord with the pQCD factorization theorem. Using Eq. (22), we obtain the finite $O(\alpha_{em})$ hard-scattering cross section

$$\begin{aligned}
E_\gamma \frac{d\hat{\sigma}_{e^+e^- \rightarrow \gamma X}^{(1)}}{d^3\ell} = & 2 \sum_q \left[\frac{2}{s} F_q^{PC}(s) \right] \left[\alpha_{em}^2 N_c \frac{1}{x_\gamma} \right] e_q^2 \left(\frac{\alpha_{em}}{2\pi} \right) \\
& \times \left\{ (1 + \cos^2\theta_\gamma) \left[\frac{1 + (1 - x_\gamma)^2}{x_\gamma} \right] [\ell n(s/\mu_{\overline{MS}}^2) + \ell n(x_\gamma^2(1 - x_\gamma))] \right. \\
& \left. + (1 - 3\cos^2\theta_\gamma) \left[\frac{2(1 - x_\gamma)}{x_\gamma} \right] \right\}. \tag{48}
\end{aligned}$$

We remark that the angular dependence of the $O(\alpha_{em})$ hard-scattering cross section has two components, one proportional to $(1 + \cos^2 \theta)$, familiar from the lowest order expression, and a second piece proportional to $(1 - 3 \cos^2 \theta_\gamma)$. If one integrates over $\cos \theta_\gamma$, the second piece vanishes. We note, however, that the piece proportional to $(1 - 3 \cos^2 \theta_\gamma)$ changes the predicted angular dependence from the often assumed form $(1 + \cos^2 \theta)$. The difference means that it would not be correct to assume a $(1 + \cos^2 \theta)$ dependence when attempting to correct an integrated cross section for unobserved events near, for example, the incident e^+e^- beam direction, $\cos \theta_\gamma = \pm 1$.

B. Derivation of $\hat{\sigma}_{e^+e^- \rightarrow gX}^{(1)}$

The finite hard-scattering cross section $\hat{\sigma}_{e^+e^- \rightarrow gX}^{(1)}$ to first order in α_s may be obtained directly from Eq. (48) after three replacements: $x_\gamma \rightarrow x_g$; $N_c \rightarrow N_c C_F$; and $e^2 e_q^2$ of the final photon emission vertex by $g^2 = 4\pi\alpha_s$.

$$E_g \frac{d\hat{\sigma}_{e^+e^- \rightarrow gX}^{(1)}}{d^3 p_g} = 2 \sum_q \left[\frac{2}{s} F_q^{PC}(s) \right] \left[\alpha_{em}^2 N_c \frac{1}{x_g} \right] C_F \left(\frac{\alpha_s}{2\pi} \right) \times \left\{ \left(1 + \cos^2 \theta_g \right) \left[\frac{1 + (1 - x_g)^2}{x_g} \right] \left[\ell n \left(s/\mu_{\overline{MS}}^2 \right) + \ell n \left(x_g^2 (1 - x_g) \right) \right] + \left(1 - 3 \cos^2 \theta_g \right) \left[\frac{2(1 - x_g)}{x_g} \right] \right\}. \quad (49)$$

In Eq. (49), $x_g = 2E_g/\sqrt{s}$; $C_F = \frac{4}{3}$, and $N_c = 3$.

The contribution $O(\alpha_s)$ to the inclusive yield $e^+e^- \rightarrow \gamma X$ via gluon fragmentation is therefore

$$E_\gamma \frac{d\sigma_{e^+e^- \rightarrow gX \rightarrow \gamma X}^{(1)}}{d^3 \ell} = \int_{x_\gamma}^1 \frac{dz}{z} \left[E_g \frac{d\hat{\sigma}_{e^+e^- \rightarrow gX}^{(1)}}{d^3 p_g} \left(x_g = \frac{x_\gamma}{z} \right) \right] \frac{D_{g \rightarrow \gamma}(z, \mu_{\overline{MS}}^2)}{z} \quad (50)$$

with $x_\gamma = 2E_\gamma/\sqrt{s}$. Because the $g \rightarrow \gamma$ fragmentation process is collinear, $\theta_g = \theta_\gamma$.

C. Derivation of $\hat{\sigma}_{e^+e^- \rightarrow qX}^{(1)}$

In this section we present our explicit derivation of the finite hard-scattering cross section $E_q \hat{\sigma}_{e^+e^- \rightarrow qX}^{(1)}/d^3 p_q$ to first order in α_s . As sketched in Fig. 6, both real gluon emission and

virtual gluon exchange graphs contribute. The real emission diagrams have both infrared and collinear divergences. The infrared divergence is cancelled by contributions from the virtual diagrams, while the collinear divergence is cancelled by the subtraction term defined in Eq. (25).

The real emission diagrams can be treated easily in the same way as $d\sigma_{e^+e^- \rightarrow \gamma X}^{(1)}/d^3\ell$ in Section III A. Except for the replacement of a photon by a gluon, the hadronic tensor $H_{\mu\nu}$ obtained from the gluon emission diagrams in Fig. 6a is identical to that computed in Section III A for $e^+e^- \rightarrow q\bar{q}\gamma$. Thus, we may employ our previous expressions for H_1 and H_2 again but with the replacement of subscript “ ℓ ” in Eqs. (30) and (34) by subscript “3”, since p_3 is our momentum label for the gluon. Because the quark is now the fragmenting particle (i.e., effectively the “observed” particle), the y_{ik}^2 variables with $i = 1, 2, 3$ in H_2 are no longer those in Eq. (38). Instead, we now have

$$\begin{aligned} y_{1k}^2 &= x_1^2 \cos^2 \theta_1 ; \\ y_{2k}^2 &= \left[\frac{y_{13}y_{23} - y_{12}}{x_1} \right]^2 \cos^2 \theta_1 + \left(\frac{1}{1-\epsilon} \right) \left[\frac{2(y_{12}y_{13}y_{23})}{x_1^2} \right] \sin^2 \theta_1 ; \\ &\text{and} \\ y_{3k}^2 &= \left[\frac{y_{12}y_{23} - y_{13}}{x_1} \right]^2 \cos^2 \theta_1 + \left(\frac{1}{1-\epsilon} \right) \left[\frac{2(y_{12}y_{13}y_{23})}{x_1^2} \right] \sin^2 \theta_1 . \end{aligned} \quad (51)$$

In Eq. (51), θ_1 is the scattering angle of the quark, and subscript “3” indicates the gluon of momentum p_3 . We dropped all terms linear in $\cos \theta_x$, and replaced $\cos^2 \theta_x$ by its average value in n -dimensions. Substituting these y_{ik}^2 with $i = 1, 2, 3$ into Eq. (34), we derive

$$\begin{aligned} \frac{1}{4} (H_1 + H_2^{eff}) &= (1 + \cos^2 \theta_1 - 2\epsilon) \left[(1 - \epsilon) \left(\frac{y_{13}}{y_{23}} + \frac{y_{23}}{y_{13}} \right) + 2 \left(\frac{y_{12}}{y_{13}y_{23}} - \epsilon \right) \right] \\ &+ (1 - 3 \cos^2 \theta_1) \left[\frac{2y_{12}}{x_1^2} \right] \\ &+ \epsilon \cos^2 \theta_1 \left[\frac{4y_{12}}{x_1^2} \right] , \end{aligned} \quad (52)$$

where the last term again vanishes as $\epsilon \rightarrow 0$. In analogy to Eq. (40), the useful identities here are

$$\begin{aligned}
y_{23} &= 1 - x_1 ; \\
y_{12} &= x_1 - y_{13} .
\end{aligned} \tag{53}$$

Using these identities, we reexpress Eq. (52) in terms of x_1 and y_{13}

$$\begin{aligned}
\frac{1}{4} (H_1 + H_2^{eff}) &= (1 + \cos^2 \theta_1 - 2\epsilon) \left\{ \left[\frac{1 + x_1^2}{1 - x_1} \right] \frac{1}{y_{13}} + \frac{y_{13}}{1 - x_1} - \frac{2}{1 - x_1} \right. \\
&\quad \left. - \epsilon \left[\frac{1 - x_1}{y_{13}} + \frac{y_{13}}{1 - x_1} + 2 \right] \right\} \\
&\quad + (1 - 3 \cos^2 \theta_1) \left[\frac{2}{x_1} \left(1 - \frac{y_{13}}{x_1} \right) \right] ,
\end{aligned} \tag{54}$$

where we dropped the last term in Eq. (52). Introducing the overall coupling factor $(e\mu^\epsilon)^2(g\mu^\epsilon)^2$ and color factor $N_c C_F$, and combining with the three particle final state phase space $dPS^{(3)}$, Eq. (A30), we express the contribution of real gluon emission as

$$\begin{aligned}
E_1 \frac{d\sigma_{e^+e^- \rightarrow qX}^{(R)}}{d^3 p_1} &= \left[\frac{2}{s} F^{PC}(s) \right] \left[\alpha_{em}^2 N_c \left(\frac{4\pi\mu^2}{(s/4)\sin^2\theta_1} \right)^\epsilon \frac{1}{\Gamma(1-\epsilon)} \right] \\
&\quad \times C_F \left(\frac{\alpha_s}{2\pi} \right) \left[\left(\frac{4\pi\mu^2}{s} \right)^\epsilon \frac{1}{\Gamma(1-\epsilon)} \right] \frac{\delta(x_1 - (1 - y_{23}))}{x_1} \\
&\quad \times \frac{1}{4} [H_1 + H_2^{eff}] \frac{dy_{12}}{y_{12}^\epsilon} \frac{dy_{13}}{y_{13}^\epsilon} \frac{dy_{23}}{y_{23}^\epsilon} \delta(1 - y_{12} - y_{13} - y_{23}) ,
\end{aligned} \tag{55}$$

where superscript (R) stands for the real emission. Using the two δ -functions to fix y_{23} and y_{12} , inserting $H_1 + H_2^{eff}$ from Eq. (54), and integrating dy_{13} from 0 to x_1 , we derive

$$\begin{aligned}
E_1 \frac{d\sigma_{e^+e^- \rightarrow qX}^{(R)}}{d^3 p_1} &= \left[\frac{2}{s} F^{PC}(s) \right] \left[\alpha_{em}^2 N_c \left(\frac{4\pi\mu^2}{(s/4)\sin^2\theta_1} \right)^\epsilon \frac{1}{\Gamma(1-\epsilon)} \right] \\
&\quad \times C_F \left(\frac{\alpha_s}{2\pi} \right) \left[\left(\frac{4\pi\mu^2}{s} \right)^\epsilon \frac{1}{\Gamma(1-\epsilon)} \right] \left(\frac{1}{x_1} \right) \frac{\Gamma(1-\epsilon)^2}{\Gamma(1-2\epsilon)} \\
&\quad \times \left\{ (1 + \cos^2 \theta_1 - 2\epsilon) \left[\left(\frac{1 + x_1^2}{(1 - x_1)_+} + \frac{3}{2} \delta(1 - x_1) \right) \left(\frac{1}{-\epsilon} \right) \right. \right. \\
&\quad \left. + \left(\frac{1 + x_1^2}{1 - x_1} \right) \ell n \left(x_1^2 \right) + \left(1 + x_1^2 \right) \left(\frac{\ell n(1 - x_1)}{1 - x_1} \right)_+ - \frac{3}{2} \left(\frac{1}{1 - x_1} \right)_+ \right. \\
&\quad \left. + \delta(1 - x_1) \left(\frac{2}{\epsilon^2} + \frac{3}{\epsilon} + \frac{7}{2} \right) - \frac{1}{2} (3x_1 - 5) \right] \\
&\quad + (1 - 3 \cos^2 \theta_1) \left. \right\} .
\end{aligned} \tag{56}$$

The “+” prescription is defined as usual

$$\left(\frac{1}{1-x_1}\right)_+ \equiv \left(\frac{1}{1-x_1}\right) - \delta(1-x_1) \int_0^1 dz \left(\frac{1}{1-z}\right). \quad (57)$$

The right-hand-side of Eq. (56) is formally divergent as $\epsilon \rightarrow 0$. The $1/\epsilon$ poles in n -dimensions represent the infrared divergence, when the gluon momentum goes to zero, and/or a collinear divergence, when the gluon momentum is parallel to that of the fragmenting quark. As we show below, the infrared divergence is cancelled by the infrared divergence of the virtual diagrams, sketched in Fig. 6b.

The contribution of the virtual diagrams results from the interference of the one-loop vertex and self-energy diagrams with the leading order tree diagram. As for the leading order contribution, the virtual diagrams, sketched in Fig. 6b, have a two-particle final state phase space. Therefore, the contribution from the virtual diagrams has the same kinematical structure and angular dependence as the leading order contribution, discussed in Section II C. It is proportional to $\delta(1-x_1)$, and, consequently, the virtual contribution cancels only the $1/\epsilon$ poles associated with the $\delta(1-x_1)$ terms in Eq. (56). The subtraction terms in Eq. (25) cancel the final state collinear poles that appear in the contribution of real gluon emission.

Beginning with the virtual exchange diagrams in Fig. 6b, we evaluate the one-loop vertex correction in n -dimension, and combine it with the lowest order tree diagram to form the first order virtual contribution. We derive

$$\begin{aligned} E_1 \frac{d\sigma_{e^+e^- \rightarrow qX}^{(V)}}{d^3 p_1} &= \left[\frac{2}{s} F^{PC}(s) \right] \left[\alpha_{em}^2 N_c \left(\frac{4\pi\mu^2}{(s/4)\sin^2\theta_1} \right)^\epsilon \frac{1}{\Gamma(1-\epsilon)} \right] \\ &\times C_F \left(\frac{\alpha_s}{2\pi} \right) \left[\left(\frac{4\pi\mu^2}{s} \right)^\epsilon \frac{1}{\Gamma(1-\epsilon)} \right] \left(\frac{1}{x_1} \right) \frac{\Gamma(1-\epsilon)^3 \Gamma(1+\epsilon)}{\Gamma(1-2\epsilon)} \\ &\times \left\{ (1 + \cos^2\theta_1 - 2\epsilon) \delta(1-x_1) \left[-\frac{2}{\epsilon^2} - \frac{3}{\epsilon} + (\pi^2 - 8) \right] \right\}, \end{aligned} \quad (58)$$

where the superscript (V) stands for the virtual contribution. After adding the real and virtual contributions, Eqs. (56) and (58), we obtain the cross section for $e^+e^- \rightarrow qX$ at order $O(\alpha_s)$,

$$\begin{aligned}
E_1 \frac{d\sigma_{e^+e^- \rightarrow qX}^{(1)}}{d^3 p_1} = & \left[\frac{2}{s} F^{PC}(s) \right] \left[\alpha_{em}^2 N_c \left(\frac{4\pi\mu^2}{(s/4)\sin^2\theta_1} \right)^\epsilon \frac{1}{\Gamma(1-\epsilon)} \right] \\
& \times C_F \left(\frac{\alpha_s}{2\pi} \right) \frac{1}{x_1} \left\{ \left(1 + \cos^2\theta_1 - 2\epsilon \right) \left[\frac{1+x_1^2}{(1-x_1)_+} + \frac{3}{2}\delta(1-x_1) \right] \left(\frac{1}{-\epsilon} \right) \right\} \\
& + \left[\frac{2}{s} F^{PC}(s) \right] \left[\alpha_{em}^2 N_c \frac{1}{x_1} \right] C_F \left(\frac{\alpha_s}{2\pi} \right) \\
& \times \left\{ \left(1 + \cos^2\theta_1 \right) \left[\left(\frac{1+x_1^2}{(1-x_1)_+} + \frac{3}{2}\delta(1-x_1) \right) \ln \left(\frac{s}{\mu_{\text{MS}}^2} \right) \right. \right. \\
& \quad + \left(\frac{1+x_1^2}{1-x_1} \right) \ln(x_1^2) + \left(1 + x_1^2 \right) \left(\frac{\ln(1-x_1)}{1-x_1} \right)_+ - \frac{3}{2} \left(\frac{1}{1-x_1} \right)_+ \\
& \quad \left. \left. + \delta(1-x_1) \left(\frac{2\pi^2}{3} - \frac{9}{2} \right) - \frac{1}{2} (3x_1 - 5) \right] \right. \\
& \quad \left. + \left(1 - 3\cos^2\theta_1 \right) \right\}. \tag{59}
\end{aligned}$$

As is evident from the $1/\epsilon$ terms, this cross section is divergent as $\epsilon \rightarrow 0$, a reflection of the fact that a cross section for producing a massless quark is an infrared sensitive quantity, not perturbatively calculable.

According to the pQCD factorization theorem, the short-distance hard-scattering cross sections, defined in Eq. (11), are infrared safe quantities. Beyond the Born level, the short-distance parts, $\hat{\sigma}_{e^+e^- \rightarrow cX}$, are not the same as the partonic cross sections $\sigma_{e^+e^- \rightarrow cX}$ for fragmenting parton c . Following Eq. (25), in order to derive the short-distance hard-scattering cross section $\hat{\sigma}_{e^+e^- \rightarrow qX}^{(1)}$, we must first calculate the one-loop perturbative fragmentation function $D_{q \rightarrow q}^{(1)}$. Feynman diagrams for $D_{q \rightarrow q}^{(1)}$ are sketched in Fig. 10. These diagrams are evaluated in the same way as one evaluates parton-level parton distributions [13], and we obtain

$$D_{q \rightarrow q}^{(1)}(x_1) = C_F \left(\frac{\alpha_s}{2\pi} \right) \left[\frac{1+x_1^2}{(1-x_1)_+} + \frac{3}{2}\delta(1-x_1) \right] \left(\frac{1}{-\epsilon} \right), \tag{60}$$

where the “+” prescription is defined in Eq. (57).

Using Eq. (25), the lowest order cross section for $e^+e^- \rightarrow qX$, Eq. (18), and the one-loop quark fragmentation function $D_{q \rightarrow q}^{(1)}$, Eq. (60), we derive the short-distance hard-scattering cross section

$$\begin{aligned}
E_1 \frac{d\hat{\sigma}_{e^+e^- \rightarrow qX}^{(1)}}{d^3 p_1} = & \left[\frac{2}{s} F_q^{PC}(s) \right] \left[\alpha_{em}^2 N_c \frac{1}{x_1} \right] C_F \left(\frac{\alpha_s}{2\pi} \right) \\
& \times \left\{ (1 + \cos^2 \theta_\gamma) \left[\left(\frac{1 + x_1^2}{(1 - x_1)_+} + \frac{3}{2} \delta(1 - x_1) \right) \ln \left(\frac{s}{\mu_{\text{MS}}^2} \right) \right. \right. \\
& + \left(\frac{1 + x_1^2}{1 - x_1} \right) \ln \left(x_1^2 \right) + \left(1 + x_1^2 \right) \left(\frac{\ln(1 - x_1)}{1 - x_1} \right)_+ - \frac{3}{2} \left(\frac{1}{1 - x_1} \right)_+ \\
& \left. \left. + \delta(1 - x_1) \left(\frac{2\pi^2}{3} - \frac{9}{2} \right) - \frac{1}{2} (3x_1 - 5) \right] \right. \\
& \left. + (1 - 3 \cos^2 \theta_\gamma) \right\}. \tag{61}
\end{aligned}$$

We set $\theta_\gamma = \theta_1$ based on the assumption of collinear fragmentation from quark to photon. As expected, the hard-scattering cross section is infrared insensitive. The $O(\alpha_s)$ quark fragmentation contribution to $e^+e^- \rightarrow \gamma X$ is

$$E_\gamma \frac{d\sigma_{e^+e^- \rightarrow qX \rightarrow \gamma X}^{(1)}}{d^3 \ell} = \sum_q \int_{x_\gamma}^1 \frac{dz}{z} \left[E_1 \frac{d\hat{\sigma}_{e^+e^- \rightarrow qX}^{(1)}}{d^3 p_1} \left(x_1 = \frac{x_\gamma}{z} \right) \right] \frac{D_{q \rightarrow \gamma}(z, \mu_{\text{MS}}^2)}{z}. \tag{62}$$

Our derivation shows that the short-distance hard-scattering cross section for antiquark fragmentation to a photon is the same as that for quark fragmentation. Consequently, the $O(\alpha_s)$ antiquark fragmentation contribution to $e^+e^- \rightarrow \gamma X$ is the same as that given in Eq. (62).

IV. NUMERICAL RESULTS AND DISCUSSION

In this section we present and discuss explicit numerical evaluations of the inclusive prompt photon cross sections derived in this paper. We provide results at e^+e^- center-of-mass energies $\sqrt{s} = 10$ GeV, 58 GeV, and 91 GeV appropriate for experimental investigations underway at Cornell, KEK, SLAC, and CERN. In our figures, we display the variation of the inclusive yield with photon energy E_γ and scattering angle θ_γ , where θ_γ is the angle of the photon with respect to the e^+e^- collision axis. We also show the dependence of cross sections on the choice of renormalization scale μ .

The cross sections we evaluate are those derived in the text: Eqs. (19), (48), (50), and (62). They are assembled here for convenience of comparison. The lowest order inclusive

cross section is

$$E_\gamma \frac{d\sigma_{e^+e^-\rightarrow\gamma X}^{incl}}{d^3\ell} = 2 \sum_q \left[\frac{2}{s} F_q^{PC}(s) \right] \alpha_{em}^2(s) N_c (1 + \cos^2 \theta_\gamma) \frac{1}{x_\gamma} D_{q\rightarrow\gamma}(x_\gamma, \mu_F^2). \quad (63)$$

The finite $O(\alpha_{em})$ hard-scattering cross section is

$$\begin{aligned} E_\gamma \frac{d\hat{\sigma}_{e^+e^-\rightarrow\gamma X}^{(1)}}{d^3\ell} = & 2 \sum_q \left[\frac{2}{s} F_q^{PC}(s) \right] \left[\alpha_{em}^2(s) N_c \frac{1}{x_\gamma} \right] e_q^2 \left(\frac{\alpha_{em}(\mu_F^2)}{2\pi} \right) \\ & \times \left\{ (1 + \cos^2 \theta_\gamma) \left[\frac{1 + (1 - x_\gamma)^2}{x_\gamma} \right] [\ell n(s/\mu_F^2) + \ell n(x_\gamma^2 (1 - x_\gamma))] \right. \\ & \left. + (1 - 3 \cos^2 \theta_\gamma) \left[\frac{2(1 - x_\gamma)}{x_\gamma} \right] \right\}. \end{aligned} \quad (64)$$

The $O(\alpha_s)$ contribution to the inclusive yield $e^+e^- \rightarrow \gamma X$ via gluon fragmentation is

$$E_\gamma \frac{d\sigma_{e^+e^-\rightarrow gX\rightarrow\gamma X}^{(1)}}{d^3\ell} = \int_{x_\gamma}^1 \frac{dz}{z} \left[E_g \frac{d\hat{\sigma}_{e^+e^-\rightarrow gX}^{(1)}}{d^3p_g} \left(x_g = \frac{x_\gamma}{z} \right) \right] \frac{D_{g\rightarrow\gamma}(z, \mu_F^2)}{z} \quad (65)$$

with

$$\begin{aligned} E_g \frac{d\hat{\sigma}_{e^+e^-\rightarrow gX}^{(1)}}{d^3p_g} = & 2 \sum_q \left[\frac{2}{s} F_q^{PC}(s) \right] \left[\alpha_{em}^2(s) N_c \frac{1}{x_g} \right] C_F \left(\frac{\alpha_s(\mu_F^2)}{2\pi} \right) \\ & \times \left\{ (1 + \cos^2 \theta_\gamma) \left[\frac{1 + (1 - x_g)^2}{x_g} \right] [\ell n(s/\mu_F^2) + \ell n(x_g^2 (1 - x_g))] \right. \\ & \left. + (1 - 3 \cos^2 \theta_\gamma) \left[\frac{2(1 - x_g)}{x_g} \right] \right\}. \end{aligned} \quad (66)$$

We choose the renormalization scale μ in $\alpha_s(\mu^2)$ to be the same as the fragmentation scale μ_F in $D_{g\rightarrow\gamma}(z, \mu_F^2)$. The $O(\alpha_s)$ contribution to the inclusive yield $e^+e^- \rightarrow \gamma X$ via quark fragmentation is

$$E_\gamma \frac{d\sigma_{e^+e^-\rightarrow qX\rightarrow\gamma X}^{(1)}}{d^3\ell} = \sum_q \int_{x_\gamma}^1 \frac{dz}{z} \left[E_1 \frac{d\hat{\sigma}_{e^+e^-\rightarrow qX}^{(1)}}{d^3p_1} \left(x_1 = \frac{x_\gamma}{z} \right) \right] \frac{D_{q\rightarrow\gamma}(z, \mu_F^2)}{z}. \quad (67)$$

with

$$\begin{aligned}
E_1 \frac{d\hat{\sigma}_{e^+e^- \rightarrow qX}^{(1)}}{d^3 p_1} = & \left[\frac{2}{s} F_q^{PC}(s) \right] \left[\alpha_{em}^2(s) N_c \frac{1}{x_1} \right] C_F \left(\frac{\alpha_s(\mu_F^2)}{2\pi} \right) \\
& \times \left\{ (1 + \cos^2 \theta_\gamma) \left[\left(\frac{1 + x_1^2}{(1 - x_1)_+} + \frac{3}{2} \delta(1 - x_1) \right) \ln \left(\frac{s}{\mu_F^2} \right) \right. \right. \\
& + \left(\frac{1 + x_1^2}{1 - x_1} \right) \ln(x_1^2) + (1 + x_1^2) \left(\frac{\ln(1 - x_1)}{1 - x_1} \right)_+ - \frac{3}{2} \left(\frac{1}{1 - x_1} \right)_+ \\
& + \delta(1 - x_1) \left(\frac{2\pi^2}{3} - \frac{9}{2} \right) - \frac{1}{2} (3x_1 - 5) \left. \right] \\
& + (1 - 3 \cos^2 \theta_\gamma) \left. \right\}. \tag{68}
\end{aligned}$$

For the common overall normalization function $F_q^{PC}(s)$, we use an expression that includes γ , Z° interference:

$$\begin{aligned}
\frac{2}{s} F_q^{PC}(s) = & \frac{1}{s^2} \left[e_q^2 + (|v_e|^2 + |a_e|^2) (|v_q|^2 + |a_q|^2) \frac{s^2}{(s - M_Z^2)^2 + M_Z^2 \Gamma_Z^2} \right. \\
& \left. + 2e_q v_e v_q \frac{s(s - M_Z^2)}{(s - M_Z^2)^2 + M_Z^2 \Gamma_Z^2} \right]. \tag{69}
\end{aligned}$$

The vector (v) and axial-vector (a) couplings are provided in Table I and Table II. We set $M_Z = 91.187$ GeV and $\Gamma_Z = 2.491$ GeV. These and other constants used here are taken from Ref. [15]. The weak mixing angle $\sin^2 \theta_w = 0.2319$. For the electromagnetic coupling strength α_{em} , we use the solution of the first order QED renormalization group equation

$$\alpha_{em}(\mu^2) = \frac{\alpha_{em}(\mu_0^2)}{1 + \frac{\beta_0}{4\pi} \alpha_{em}(\mu_0^2) \ln(\mu^2/\mu_0^2)}. \tag{70}$$

Here β_0 is the first order QED beta function,

$$\beta_0 = -\frac{4}{3} \sum_f N_c^f e_f^2, \tag{71}$$

with N_c^f the number of colors for flavor f and e_f the fractional charge of the fermions. The sum over f extends over all fermions (leptons and quarks) with mass $m_f^2 < \mu^2$. For the energy region of interest here, we do not include the top quark in the sum in Eq. (71), and we obtain $\beta_0 = -80/9$. To fix the boundary condition in Eq. (70), we let $\alpha_{em}(M_Z^2) = 1/128$ and set $\mu_0 = M_Z$.

In the $O(\alpha_s)$ contributions, Eqs. (66) and (68), we employ a two-loop expression for $\alpha_s(\mu^2)$ with quark threshold effects handled properly. We set $\Lambda_{QCD}^{(4)} = 0.231$ GeV. At $\sqrt{s} = M_Z$, this expression provides $\alpha_s(M_Z^2) = 0.112$.

At $\sqrt{s} = 10$ GeV, the sums in Eqs. (64), (66), and (68) run over 4 flavors of quarks (u, d, c, s), all assumed massless. At this energy, we do not include a b quark contribution in our calculation. For $\sqrt{s} = 58$ GeV and 91 GeV, we use 5 flavors, again assuming all massless in the short-distance hard scattering cross sections. At these higher energies, non-zero mass effects for the c and b quarks are accommodated by our scale choice in the fragmentation functions, discussed below.

The quark-to-photon fragmentation function that appears in Eq. (63) and (68) is expressed as

$$z D_{q \rightarrow \gamma}(z, \mu_F^2) = \frac{\alpha_{em}(\mu_F^2)}{2\pi} \left[e_q^2 \frac{2.21 - 1.28z + 1.29z^2}{1 - 1.63 \ln(1-z)} z^{0.049} + 0.002 (1-z)^2 z^{-1.54} \right] \times \ln(\mu_F^2/\mu_0^2). \quad (72)$$

The gluon-to-photon fragmentation function in Eq. (65) is

$$z D_{g \rightarrow \gamma}(z, \mu_F^2) = \frac{\alpha_{em}(\mu_F^2)}{2\pi} 0.0243 (1-z) z^{-0.97} \ln(\mu_F^2/\mu_0^2). \quad (73)$$

These expressions for $D_{q \rightarrow \gamma}$ and $D_{g \rightarrow \gamma}$, taken from Ref. [14], are used as a guideline for our estimates. The physical significance of scale μ_0 is that the fragmentation function vanishes for energies less than μ_0 . For g and for the u, d, s , and c quarks, we set $\mu_0 = \Lambda_{QCD}^{(4)}$, as in Ref. [14]. For the b quark we again use Eq. (72), but we replace μ_0 by the mass of the quark, $m_b = 5$ GeV; $D_{b \rightarrow \gamma}(z, \mu_F^2) = 0$ for $\mu_F < m_b$. We set the fragmentation scale μ_F equal to the renormalization scale μ for our inclusive cross sections. In the results presented below, we vary μ to examine the sensitivity of the cross section to its choice.

In presenting results, we divide our inclusive cross sections by an energy dependent cross section σ_0 that specifies the leading order total hadronic event rate at each value of \sqrt{s} :

$$\sigma_0 = \frac{4\pi s}{3} \sum_q \left[\frac{2}{s} F_q^{PC}(s) \alpha_{em}^2(s) N_c \right]. \quad (74)$$

By doing so, we can observe what fraction of the total hadronic rate is represented by inclusive prompt photon production.

In several figures to follow, we show the predicted behavior of the inclusive yield as a function of E_γ and θ_γ , as well as the breakdown of the total yield into contributions from various components.

In Fig. 11, we present the inclusive yield as a function of E_γ at $\sqrt{s} = 91$ GeV for two values of the scattering angle θ_γ , 45° and 90° . The same results are displayed in Fig. 12 as a function of scattering angle θ_γ for two choices of E_γ . In both Figs. 11 and 12, we set renormalization/fragmentation scale $\mu = E_\gamma$. Dependence of the cross sections on μ is examined in Fig. 13 at fixed E_γ . The patterns evident in Figs. 11–13 at $\sqrt{s} = 91$ GeV are repeated with subtle differences in Figs. 14–16 at $\sqrt{s} = 58$ GeV, appropriate for experiments at TRISTAN, and in Figs. 17–19 at $\sqrt{s} = 10$ GeV, applicable for studies at CESR/CLEO. In Fig. 20 we compare predictions at the three energies by showing the cross section $\sigma_0^{-1} d\sigma/dx_\gamma d\Omega_\gamma$ as a function of the scaling variable $x_\gamma = 2E_\gamma/\sqrt{s}$.

Evident in Figs. 11–19 is the dominance of the lowest-order contribution to the inclusive yield, Eq. (63), at all values of \sqrt{s} , except at small values of E_γ/\sqrt{s} or at small values of μ where the $O(\alpha_{em})$ “direct” contribution, Eq. (64), becomes larger. Following the lowest-order contribution in importance at modest values of E_γ/\sqrt{s} or of μ is the $O(\alpha_{em})$ direct contribution. The direct contribution falls away more rapidly with increasing E_γ or μ than the $O(\alpha_s)$ quark-to-photon fragmentation term, Eq. (68). Therefore, at large values of E_γ/\sqrt{s} or μ , it is the $O(\alpha_s)$ fragmentation term, that is secondary in importance to the lowest-order term. The gluon-to-photon fragmentation contribution, Eq. (65) plays an insignificant role except at very small E_γ .

In Figs. 12, 15, and 18, we examine the predicted θ_γ dependence of our cross sections. These figures, presented with a linear scale, show perhaps more clearly the importance of the roles of the $O(\alpha_{em})$ direct and $O(\alpha_s)$ fragmentation contributions. The lowest-order contribution, Eq. (63), is proportional to $(1 + \cos^2 \theta_\gamma)$. However, there are significant $\sin^2 \theta_\gamma$ components in the next-to-leading order direct term, Eq. (64), and the next-to-leading order

fragmentation terms, Eqs. (66) and (68). The net result is that the predicted total yield in Figs. 12, 15, and 18 is not proportional to $(1 + \cos^2 \theta_\gamma)$. As illustrated in the figures, the deviation of the total yield from the $(1 + \cos^2 \theta_\gamma)$ form becomes greater at smaller values of E_γ . (The results shown in Figs. 12, 15, and 18 all pertain to the scale choice $\mu = E_\gamma$.) One lesson from this examination of dependence of θ_γ is that it is inappropriate and potentially misleading to assume that the functional form $(1 + \cos^2 \theta_\gamma)$ describes the data when attempts are made to correct distributions in the region of small θ_γ (where initial state bremsstrahlung overwhelms the final state radiation in which one is interested).

Dependence on the renormalization/factorization scale μ in Figs. 13, 16, and 19 shows several interesting features. As is expected from the functional form of $D_{q \rightarrow \gamma}(z, \mu^2)$ in Eq. (72), the lowest-order contribution, Eq. (63), increases logarithmically as μ is increased. On the other hand, the $\ln(s/\mu^2)$ dependent term in Eq. (64) causes a decrease of the $O(\alpha_{em})$ direct contribution as μ is increased. Indeed, the $(1 + \cos^2 \theta_\gamma)$ part of the direct contribution becomes negative when $s x_\gamma^2 (1 - x_\gamma) / \mu^2 < 1$. The physical cross section, represented as a solid line in Figs. 13, 16, and 19, is of course always positive.

An especially noteworthy feature of Figs. 13, 16, and 19 is that the total inclusive yield is nearly independent of μ , in spite of the strong variation with μ of its components. This independence reflects the role of the fragmentation scale μ . It is introduced to separate “soft” and “hard” contributions into “fragmentation” and “direct” pieces. As the scale μ is increased, more of the cross section is necessarily factored into the fragmentation contribution, and vice versa, such that the sum remains nearly constant.

In Fig. 20, we show the overall \sqrt{s} dependence of our predictions. To facilitate comparison, we present these results in terms of the “scaling” distribution $\sigma_0^{-1} d\sigma/dx_\gamma d\Omega_\gamma$. The case of $\sqrt{s} = 10$ GeV is somewhat special since we do not include a contribution from b quark fragmentation at this energy. Otherwise, the contribution of the lowest-order process, Eq. (63), decreases at fixed x_γ as \sqrt{s} is increased. This decrease is explained easily. In computing $d\sigma/dx_\gamma d\Omega_\gamma$, we multiply Eqs. (69) and (72), obtaining a charge weighting factor of

$e_q^2 F_q^{PC}(s)$, whereas in computing the denominator σ_0 , the factor is $F_q^{PC}(s)$. Owing to the values of the v and a couplings in Table 1, the up-type quark contribution to $F_q^{PC}(s)$ decreases as \sqrt{s} increases, and the down-type contribution increases. The $O(\alpha_{em})$ direct contribution to $\sigma_0^{-1} d\sigma/dx_\gamma d\Omega_\gamma$ decreases at fixed x_γ as \sqrt{s} is increased from 10 to 91 GeV. Again, the explanation may be found in the energy dependence of the ratio $\sum_q e_q^2 F_q^{PC}(s) / \sum_q F_q^{PC}(s)$. Taken together these statements explain the energy dependence displayed in Fig. 20.

As remarked earlier, the particular expressions we chose for the fragmentation functions are not meant to be anything but illustrative expressions. It would be very valuable if these non-perturbative functions could be determined directly from data. Dominance of the $q \rightarrow \gamma$ fragmentation contribution in Figs. 11–19 demonstrates the important role data from $e^+e^- \rightarrow \gamma X$ may play in the extraction of $D_{q \rightarrow \gamma}(z, \mu^2)$ and study of its properties. However, as mentioned in the Introduction, an important limitation of high energy investigations is that photons are observed and cross sections are measured reliably only when the photons are relatively isolated. Since fragmentation is a process in which photons are part of quark, antiquark, and gluon jets, isolation reduces the contribution from fragmentation terms. In a forthcoming paper [8], we will examine in detail the behavior of the isolated prompt photon cross section.

In this paper we have presented a unified treatment of inclusive prompt photon production in hadronic final states in e^+e^- annihilation. We have computed analytically the direct photon contribution through $O(\alpha_{em})$ and the quark-to-photon and gluon-to-photon fragmentation terms through $O(\alpha_s)$. We presented the full angular dependence of the cross section, separated into transverse ($1 + \cos^2 \theta_\gamma$) and longitudinal components.

ACKNOWLEDGEMENTS

X. Guo and J. Qiu are grateful for the hospitality of Argonne National Laboratory where a part of this work was completed. Work in the High Energy Physics Division at Argonne National Laboratory is supported by the U.S. Department of Energy, Division of High Energy

Physics, Contract W-31-109-ENG-38. The work at Iowa State University was supported in part by the U.S. Department of Energy under Grant Nos. DE-FG02-87ER40731 and DE-FG02-92ER40730.

APPENDIX A: TWO AND THREE PARTICLE PHASE SPACE

In this Appendix, we express two- and three-particle final state phase space $dPS^{(2)}$ and $dPS^{(3)}$ in n dimensions in terms of the variables necessary for our calculation. We work out first the specific case of $e^+e^- \rightarrow q\bar{q}$. The four-vector momenta of q and \bar{q} are p_q and $p_{\bar{q}}$.

The two particle phase space element in $n = 4 - 2\epsilon$ dimensions is

$$dPS^{(2)} = \frac{d^{n-1}p_q}{(2\pi)^{n-1}2E_q} \cdot \frac{d^{n-1}p_{\bar{q}}}{(2\pi)^{n-1}2E_{\bar{q}}} \cdot (2\pi)^n \delta^{(n)}(q - p_q - p_{\bar{q}}). \quad (\text{A1})$$

In the center of mass frame, $\vec{p}_q = -\vec{p}_{\bar{q}}$ and $E_q = E_{\bar{q}}$. Eliminating the $d^{n-1}p_{\bar{q}}$ integration, we obtain

$$dPS^{(2)} = \left(\frac{1}{2\pi}\right)^{n-2} \frac{1}{8} E_q^{n-4} dE_q d\theta \sin^{n-3} \theta d\Omega_{n-3}(p_q) \delta\left(E_q - \frac{1}{2}\sqrt{s}\right). \quad (\text{A2})$$

Since the square of the invariant matrix element, Eq. (17) of the text, depends on θ but not on other angles, we may perform the integration over $d\Omega_{n-3}$;

$$\Omega_{n-3} = 2\pi \pi^{-\epsilon} / \Gamma(1 - \epsilon). \quad (\text{A3})$$

We derive

$$dPS^{(2)} = \frac{1}{2} \frac{1}{(2\pi)^3} \frac{d^3p_q}{E_q} \left[\left(\frac{4\pi}{(s/4) \sin^2 \theta} \right)^\epsilon \frac{1}{\Gamma(1 - \epsilon)} \right] \frac{2\pi}{s} \frac{\delta(x_q - 1)}{x_q}, \quad (\text{A4})$$

with $x_q = 2E_q/\sqrt{s}$.

For the three particle final state $e^+e^- \rightarrow q\bar{q}\gamma$, we label the four-vector momenta of q, \bar{q} , and γ as p_1, p_2 , and ℓ . The invariant matrix element of interest to us, as defined in Eqs. (30) and (34), depends explicitly on the inner products $p_1 \cdot \ell, p_2 \cdot \ell$, and $p_1 \cdot p_2$ as well as on $p_1 \cdot k, p_2 \cdot k$, and $\ell \cdot k$ where k , defined in Eq. (7), is the difference $k = k_{e^+} - k_{e^-}$ of the four-momenta of the initial e^+ and e^- . However, all these inner products are not independent.

Using momentum conservation and the fact that the momenta ℓ and k are observables, one may show that $p_1 \cdot \ell$ and $p_2 \cdot k$ are the only independent invariants. Note that it is completely equivalent to choose p_2 instead of p_1 .

For general orientation, it is useful to begin in $n = 4$ dimensions to establish the angular variables of integration we would use in that case, before generalizing to n dimensions. In the overall e^+e^- center of mass frame, we imagine a coordinate system with the γ defining the z axis, vector \vec{k} lying in the (x, z) plane, and vector \vec{p}_1 generally having non-zero x, y and z components.

$$\vec{k} = |\vec{k}| (\sin \theta_\gamma, 0, \cos \theta_\gamma); \quad (\text{A5})$$

$$\vec{p}_1 = |\vec{p}_1| (\sin \theta_{1\gamma} \cos \phi, \sin \theta_{1\gamma} \sin \phi, \cos \theta_{1\gamma}); \quad (\text{A6})$$

$$\begin{aligned} p_1 \cdot k &= -\vec{p}_1 \cdot \vec{k} \\ &= -|\vec{p}_1| |\vec{k}| (\sin \theta_\gamma \sin \theta_{1\gamma} \cos \phi + \cos \theta_\gamma \cos \theta_{1\gamma}). \end{aligned} \quad (\text{A7})$$

The four-dimensional example shows that only the components of \vec{p}_1 in the $\vec{\ell}, \vec{k}$ plane contribute to $\vec{p} \cdot \vec{k}$. We use θ_x to denote the n -dimensional generalization of the four-dimensional azimuthal angular variable ϕ , and we will express $dPS^{(3)}$ in n -dimensions in terms of integrations over $\theta_{1\gamma}$ and θ_x .

Three particle phase space in n -dimensions is

$$dPS^{(3)} = \frac{d^{n-1}p_1}{(2\pi)^{n-1}2E_1} \frac{d^{n-1}p_2}{(2\pi)^{n-1}2E_2} \frac{d^{n-1}\ell}{(2\pi)^{n-1}2E_\gamma} (2\pi)^n \delta^{(n)}(q - p_1 - p_2 - \ell). \quad (\text{A8})$$

Using the $\delta^{(n)}$ function to eliminate the integrations over p_2 , we obtain

$$dPS^{(3)} = \frac{d^{n-1}p_1}{(2\pi)^{n-1}2E_1} \frac{d^{n-1}\ell}{(2\pi)^{n-1}2E_\gamma} \frac{1}{2E_2} 2\pi \delta(\sqrt{s} - E_\gamma - E_1 - E_2). \quad (\text{A9})$$

Since we are interested ultimately in the invariant cross section $E_\gamma d\sigma/d^3\ell$, we rewrite Eq. (A9) as follows.

$$\begin{aligned} \frac{d^{n-1}\ell}{(2\pi)^{n-1}2E_\gamma} &= \frac{1}{(2\pi)^{n-1}2E_\gamma} E_\gamma^{n-2} dE_\gamma d\theta_\gamma \sin^{n-3} \theta_\gamma d\Omega_{n-3}(\ell) \\ &\equiv \frac{1}{2} \frac{1}{(2\pi)^3} \frac{d^3\ell}{E_\gamma} \frac{1}{(2\pi)^{n-4}} (E_\gamma^2 \sin^2 \theta_\gamma)^{\frac{n-4}{2}} \frac{d\Omega_{n-3}(\ell)}{d\phi_\gamma}. \end{aligned} \quad (\text{A10})$$

We take angle θ_γ to be the polar angle of the γ with respect to the e^+e^- collision axis in the overall center of mass frame. Since the square of the matrix element does not depend on ϕ_γ , we can integrate over $d\Omega_{n-3}(\ell)$ and $d\phi_\gamma$ independently. Using Ω_{n-3} from Eq. (A3), and $\int d\phi_\gamma = 2\pi$, we reexpress Eq. (A10) as

$$\frac{d^{n-1}\ell}{(2\pi)^{n-1}2E_\gamma} = \frac{1}{2} \frac{1}{(2\pi)^3} \frac{d^3\ell}{E_\gamma} \left[\left(\frac{4\pi}{E_\gamma^2 \sin^2 \theta_\gamma} \right)^\epsilon \frac{1}{\Gamma(1-\epsilon)} \right]. \quad (\text{A11})$$

We write $d^{n-1}p_1$ in Eq. (A9) as

$$\begin{aligned} d^{n-1}p_1 &= E_1^{n-2} dE_1 d\Omega_{n-2}(p_1) \\ &= E_1^{n-2} dE_1 d\theta_{1\gamma} \sin^{n-3} \theta_{1\gamma} d\Omega_{n-3}(p_1), \end{aligned} \quad (\text{A12})$$

with

$$\begin{aligned} d\Omega_{n-3}(p_1) &= d\theta_x \sin^{n-4} \theta_x d\Omega_{n-4}(p_1) \\ &= d\cos \theta_x (1 - \cos^2 \theta_x)^{\frac{n-5}{2}} d\Omega_{n-4}(p_1) \end{aligned} \quad (\text{A13})$$

Since only the components of p_1 in the $\vec{\ell}, \vec{k}$ plane contribute to $p_1 \cdot k$, as shown in Eq. (A7), all angular variables on which the invariant matrix element depends are displayed explicitly in Eqs. (A12) and (A13). We may therefore integrate $d\Omega_{n-4}(p_1)$ in Eq. (A13) to obtain

$$\Omega_{n-4}(p_1) = \frac{2^{n-4} \pi^{\frac{n-4}{2}} \Gamma(\frac{n-4}{2})}{\Gamma(n-4)}. \quad (\text{A14})$$

In this frame, E_2 in Eq. (A9) can be expressed as

$$E_2^2 = (\vec{p}_2)^2 = (\vec{p}_1 + \vec{\ell})^2 = E_1^2 + E_\gamma^2 + 2E_1 E_\gamma \cos \theta_{1\gamma}. \quad (\text{A15})$$

Using Eq. (A15), we can replace the integration over $d\cos \theta_{1\gamma}$ in Eq. (A12) by an integration over dE_2 ; for fixed E_1 ,

$$E_1 E_\gamma d\cos \theta_{1\gamma} = E_2 dE_2. \quad (\text{A16})$$

Substituting into Eq. (A9), we derive

$$\begin{aligned}
dPS^{(3)} = & \frac{1}{2} \frac{1}{(2\pi)^3} \frac{d^3\ell}{E_\gamma} \left[\left(\frac{4\pi}{E_\gamma^2 \sin^2 \theta_\gamma} \right)^\epsilon \frac{1}{\Gamma(1-\epsilon)} \right] \\
& \times \frac{1}{4} \frac{1}{(2\pi)^2} \left(\frac{4\pi^2}{E_1^2 \sin^2 \theta_{1\gamma}} \right)^\epsilon \Omega_{n-4}(p_1) (1 - \cos^2 \theta_x)^{-\epsilon-1/2} d\cos \theta_x \\
& \times \frac{1}{E_\gamma} \delta(\sqrt{s} - E_\gamma - E_1 - E_2) dE_1 dE_2. \tag{A17}
\end{aligned}$$

It is easy to verify that Eq. (A17) reduces to the familiar form in four-dimensions when $\epsilon \rightarrow 0$.

We introduce new dimensionless variables related to the singularity structure of the invariant matrix elements, given in Eqs. (30) and (34):

$$y_{12} \equiv \frac{2p_1 \cdot p_2}{q^2} \tag{A18a}$$

$$y_{1\ell} \equiv \frac{2p_1 \cdot \ell}{q^2} \tag{A18b}$$

$$y_{2\ell} \equiv \frac{2p_2 \cdot \ell}{q^2} \tag{A18c}$$

$$x_1 \equiv \frac{2p_1 \cdot q}{q^2} \tag{A18d}$$

$$x_2 \equiv \frac{2p_2 \cdot q}{q^2} \tag{A18e}$$

$$x_\gamma \equiv \frac{2\ell \cdot q}{q^2} \tag{A18f}$$

We observe that $y_{1\ell} = 1 - x_2$, $y_{2\ell} = 1 - x_1$, and $y_{12} = 1 - x_\gamma$. In the center of mass frame, $q = (\sqrt{s}, \vec{0})$, we have

$$x_1 = \frac{2E_1}{\sqrt{s}}, \quad \text{and} \quad x_2 = \frac{2E_2}{\sqrt{s}}; \tag{A19}$$

$$dE_1 dE_2 = \frac{s}{4} dx_1 dx_2 = \frac{s}{4} dy_{1\ell} dy_{2\ell}; \tag{A20}$$

$$\delta(\sqrt{s} - E_q - E_{\bar{q}} - E_\gamma) = \frac{2}{\sqrt{s}} \delta(1 - y_{1\ell} - y_{2\ell} - y_{12}). \tag{A21}$$

After some algebra, one may verify that

$$E_1^2 E_\gamma^2 \sin^2 \theta_{1\gamma} = \frac{s^2}{4} y_{1\ell} y_{2\ell} y_{12}. \tag{A22}$$

Substituting Eqs. (A20)-(A22) into Eq. (A17), we derive

$$\begin{aligned}
dPS^{(3)} = & \frac{1}{2} \frac{1}{(2\pi)^3} \frac{d^3\ell}{E_\gamma} \left[\left(\frac{4\pi}{(s/4) \sin^2 \theta_\gamma} \right)^\epsilon \frac{1}{\Gamma(1-\epsilon)} \right] \frac{1}{x_\gamma} \\
& \times \frac{1}{4} \frac{1}{(2\pi)^2} \left(\frac{4\pi^2}{s} \right)^\epsilon \Omega_{n-4}(p_1) (1 - \cos^2 \theta_x)^{-\epsilon-1/2} d \cos \theta_x \\
& \times \frac{dy_{1\ell} dy_{2\ell} \delta(1 - y_{1\ell} - y_{2\ell} - y_{12})}{(y_{1\ell} y_{2\ell} y_{12})^\epsilon}. \tag{A23}
\end{aligned}$$

For reference, we record that

$$\int_{-1}^1 d \cos \theta_x (1 - \cos^2 \theta_x)^{-\epsilon-1/2} = \frac{\Gamma(\frac{1}{2}) \Gamma(\frac{1}{2} - \epsilon)}{\Gamma(1 - \epsilon)} \tag{A24}$$

$$\int_{-1}^1 d \cos \theta_x \cos^2 \theta_x (1 - \cos^2 \theta_x)^{-\epsilon-1/2} = \frac{\Gamma(\frac{3}{2}) \Gamma(\frac{1}{2} - \epsilon)}{\Gamma(2 - \epsilon)}. \tag{A25}$$

Dividing Eq. (A25) by Eq. (A24), we define the average of $\cos^2 \theta_x$ in n -dimensions as

$$\langle \cos^2 \theta_x \rangle = \frac{1}{2} \frac{1}{1 - \epsilon}. \tag{A26}$$

When $\epsilon \rightarrow 0$, θ_x becomes the azimuthal angular ϕ , and Eq. (A26) is consistent with the 4-dimensional result

$$\langle \cos^2 \phi \rangle \equiv \frac{1}{2\pi} \int_0^{2\pi} d\phi \cos^2 \phi = \frac{1}{2}. \tag{A27}$$

Equation (A23) is written in a form for which the photon with momentum ℓ is the observed particle, with integrations done over the momenta of other final state partons. When considering $e^+e^- \rightarrow q\bar{q}g$ with q (or \bar{q}) fragmenting into the observed γ , we require instead $E_q d\sigma/d^3p_q$. It is useful, therefore, to reexpress Eq. (A23) in a form that manifests the symmetry of phase space among all three final state particles.

Using $y_{12} = 1 - x_\gamma$, we introduce the identity

$$1 = dy_{12} \delta(x_\gamma - (1 - y_{12})). \tag{A28}$$

Inserting this identity into Eq. (A23), we obtain a more symmetric form

$$\begin{aligned}
dPS^{(3)} = & \frac{1}{2} \frac{1}{(2\pi)^3} \frac{d^3\ell}{E_\gamma} \left[\left(\frac{4\pi}{(s/4) \sin^2 \theta_\gamma} \right)^\epsilon \frac{1}{\Gamma(1-\epsilon)} \right] \frac{2\pi}{s} \frac{\delta(x_\gamma - (1 - y_{12}))}{x_\gamma} \\
& \times \frac{s}{4} \left[\left(\frac{1}{2\pi} \right)^2 \left(\frac{4\pi}{s} \right)^\epsilon \frac{1}{\Gamma(1-\epsilon)} \frac{d\Omega_{n-3}(p_1)}{\Omega_{n-3}(p_1)} \right] \\
& \times \frac{dy_{1\ell}}{y_{1\ell}^\epsilon} \frac{dy_{2\ell}}{y_{2\ell}^\epsilon} \frac{dy_{12}}{y_{12}^\epsilon} \delta(1 - y_{1\ell} - y_{2\ell} - y_{12}) . \tag{A29}
\end{aligned}$$

We can use Eq. (A29) to derive an expression for three-particle phase-space suitable for calculating $E_q d\sigma/d^3p_q$ when the quark from $e^+e^- \rightarrow q\bar{q}g$ is the fragmenting parton. We label (q, \bar{q}, g) as $(1, 2, 3)$. We let the gluon replace the photon γ in Eq. (A29), and we then switch the labels of the g and the observed quark. We derive

$$\begin{aligned}
dPS^{(3)} = & \frac{1}{2} \frac{1}{(2\pi)^3} \frac{d^3p_1}{E_1} \left[\left(\frac{4\pi}{(s/4) \sin^2 \theta_1} \right)^\epsilon \frac{1}{\Gamma(1-\epsilon)} \right] \frac{2\pi}{s} \frac{\delta(x_1 - (1 - y_{23}))}{x_1} \\
& \times \frac{s}{4} \left[\left(\frac{1}{2\pi} \right)^2 \left(\frac{4\pi}{s} \right)^\epsilon \frac{1}{\Gamma(1-\epsilon)} \frac{d\Omega_{n-3}(p_3)}{\Omega_{n-3}(p_3)} \right] \\
& \times \frac{dy_{12}}{y_{12}^\epsilon} \frac{dy_{13}}{y_{13}^\epsilon} \frac{dy_{23}}{y_{23}^\epsilon} \delta(1 - y_{12} - y_{13} - y_{23}) . \tag{A30}
\end{aligned}$$

The first line of Eq. (A30) is identical to $dPS^{(2)}$, Eq. (A4). By switching 1 and 2 in Eq. (A30), one can get a form for the phase space suitable for calculating the hard-scattering cross section when the antiquark is the fragmenting parton.

REFERENCES

- [1] G. Altarelli, R. K. Ellis, G. Martinelli, and S. Y. Pi, Nucl. Phys. **B160**, 301 (1979); G. Gurci, W. Furmanski, and R. Petronzio, Nucl. Phys. **B175**, 27 (1980); J.C. Collins, D.E. Soper and G. Sterman, in *Perturbative Quantum Chromodynamics*, edited by A.H. Mueller (World Scientific, Singapore, 1989).
- [2] E. Witten, Nucl. Phys. **B120**, 189 (1977); R. J. DeWitt *et al.*, Phys. Rev. **D19**, 2046 (1979) and Erratum, **D20**, 1751 (1979); T. F. Walsh and P. Zerwas, Phys. Lett. **B44**, 195 (1973).
- [3] E. L. Berger, X. Guo, and J.-W. Qiu, in DPF '92, Proceedings of the 7th Meeting of the APS Division of Particles and Fields, Fermilab, November, 1992; ed. by C. H. Albright *et al.* (World Scientific, Singapore, 1993), Vol. 2, pp. 957-960.
- [4] E. L. Berger, E. Braaten, and R. D. Field, Nucl. Phys. **B239**, 52 (1984).
- [5] P. Aurenche *et al.* Phys Lett. **140B**, 87 (1984); P. Aurenche *et al.* Nucl. Phys. **B297**, 661 (1988); A. P. Contogouris, S. Papadopoulos, and D. Atwood, Theor. Math. Phys. **87**, 374 (1991); H. Baer, J. Ohnemus, and J. F. Owens, Phys. Rev. **D42**, 61 (1990); B. Bailey, J. Ohnemus, and J. F. Owens, Phys. Rev. **D46**, 2018 (1992); L. E. Gordon and W. Vogelsang, Phys. Rev. **D48**, 3136 (1993) and **D50**, 1901 (1994); M. Glück, L. E. Gordon, E. Reya, and W. Vogelsang, Phys. Rev. Lett. **73**, 388 (1994).
- [6] E. L. Berger and J.-W. Qiu, Phys. Lett. **B248**, 371 (1990); E. L. Berger and J.-W. Qiu, Phys. Rev. **D44**, 2002 (1991).
- [7] F. Abe *et al.*, CDF Collaboration, Phys. Rev. Lett. **73**, 2662 (1994); S. Fahey *et al.*, D0 Collaboration, Proceedings of the 8th Meeting of the APS Division of Particles and Fields, Albuquerque, August 1994. Edited by S. Seidel (World Scientific, Singapore, 1995). pp. 1804-1809.
- [8] E. L. Berger, X. Guo, and J.-W. Qiu, Argonne Preprint, ANL-HEP-PR-95-48.

[9] E. W. N. Glover and A. G. Morgan, Z. Phys. **C62**, 311 (1994).

[10] G. Kramer and B. Lampe, Z. Phys. **C34**, 497 (1987); Phys. Lett. **B269**, 401 (1991).
 G. Kramer and H. Spiesberger, Proceedings of Annecy Workshop on Photon Radiation from Quarks, Annecy, France, December 1991. CERN report CERN 92-04, edited by S. Cartwright. pp. 26-40.

[11] P. Mättig, H. Spiesberger, and W. Zeuner, Z. Phys. **C60**, 613 (1993).

[12] P. D. Acton *et al.*, OPAL Collaboration, Z. Phys. **C58**, 405 (1993); D. Buskulic *et al.*, ALEPH Collaboration, Z. Phys. **C57**, 17 (1993); P. Abreu *et al.*, DELPHI Collaboration, Z. Phys. **C53**, 555 (1992); O. Adriani *et al.*, L3 Collaboration, Phys. Lett. **B292**, 472 (1992).

[13] J. C. Collins and J.-W. Qiu, Phys. Rev. **D39**, 1398 (1989).

[14] J. F. Owens, Rev. Mod. Phys. **59**, 465 (1987).

[15] Particle Data Group, Phys. Rev. **D50**, 1173 (1994).

FIGURES

FIG. 1. Illustration of $e^+e^- \rightarrow \gamma X$ in an m parton state: $e^+e^- \rightarrow cX$ followed by fragmentation $c \rightarrow \gamma X$.

FIG. 2. Contribution to the hard-scattering cross section for $e^+e^- \rightarrow cX$ with the fragmentation of $c \rightarrow \gamma X$. Here c denotes an intermediate photon or a gluon or a quark of any flavor.

FIG. 3. Lowest order, $O(\alpha_{em}^o \alpha_s^o)$, photon production through quark fragmentation.

FIG. 4. Feynman diagrams for $e^+e^- \rightarrow \gamma q\bar{q}$.

FIG. 5. Order α_s Feynman diagrams for $e^+e^- \rightarrow q\bar{q}g$ that contribute to $e^+e^- \rightarrow \gamma X$ via $g \rightarrow \gamma$ fragmentation.

FIG. 6. Contributions to the $O(\alpha_s)$ cross section $\sigma_{e^+e^- \rightarrow qX}^{(1)}$; (a) real gluon emission diagrams ($e^+e^- \rightarrow q\bar{q}g$), (b) virtual gluon exchange diagrams that interfere with the lowest order tree diagram.

FIG. 7. Order $O(\alpha_{em}^2)$ contribution to the hadronic tensor $H_{\mu\nu}$.

FIG. 8. Center of mass coordinate axes of an e^+e^- collision with the z -axis being the direction of the observed photon.

FIG. 9. Feynman diagram for $D_{q \rightarrow \gamma}^{(1)}(z)$.

FIG. 10. Feynman diagrams for $D_{q \rightarrow q}^{(1)}(z)$.

FIG. 11. Normalized invariant cross section for the inclusive process $e^+e^- \rightarrow \gamma X$ at $\sqrt{s} = 91$ GeV shown as a function of the photon energy E_γ for two values of the photon scattering angles: a) $\theta_\gamma = 45^0$, and b) $\theta_\gamma = 90^0$. Displayed are the total result and the four separate contributions from lowest-order fragmentation (“oth-frag”), $O(\alpha_{em})$ direct production, and the $O(\alpha_s)$ quark and gluon fragmentation contributions. The renormalization/fragmentation scale $\mu = E_\gamma$.

FIG. 12. Normalized invariant cross section for the inclusive process $e^+e^- \rightarrow \gamma X$ at $\sqrt{s} = 91$ GeV shown as a function of the photon scattering angle θ_γ for two values of the photon energy: a) $E_\gamma = 15$ GeV, and b) $E_\gamma = 30$ GeV. The total result and the four separate component pieces are displayed. The renormalization/fragmentation scale $\mu = E_\gamma$.

FIG. 13. Renormalization/factorization scale dependence of the normalized invariant cross section for the inclusive process $e^+e^- \rightarrow \gamma X$ at $\sqrt{s} = 91$ GeV for two values of the photon scattering angle: a) $\theta_\gamma = 45^0$, and b) $\theta_\gamma = 90^0$. The photon energy $E_\gamma = 15$ GeV. The total result shows little μ dependence, whereas the component contributions display considerable compensating variation with μ .

FIG. 14. Photon energy dependence, as in Fig. 11, but for center-of-mass energy $\sqrt{s} = 58$ GeV.

FIG. 15. Photon scattering angle dependence, as in Fig. 12, but for center-of-mass energy $\sqrt{s} = 58$ GeV, and photon energies a) $E_\gamma = 10$ GeV, and b) $E_\gamma = 20$ GeV.

FIG. 16. Renormalization/factorization scale dependence, as in Fig. 13, but for center-of-mass energy $\sqrt{s} = 58$ GeV, and photon energy $E_\gamma = 10$ GeV.

FIG. 17. Photon energy dependence, as in Figs. 11 and 14, but for center-of-mass energy $\sqrt{s} = 10$ GeV.

FIG. 18. Photon scattering angle dependence, as in Figs. 12 and 15, but for center-of-mass energy $\sqrt{s} = 10$ GeV, and photon energies a) $E_\gamma = 1.5$ GeV, and b) $E_\gamma = 3$ GeV.

FIG. 19. Renormalization/factorization scale dependence, as in Figs. 13 and 16, but for center-of-mass energy $\sqrt{s} = 10$ GeV, and photon energy $E_\gamma = 2$ GeV.

FIG. 20. Normalized invariant cross section for the inclusive process $e^+e^- \rightarrow \gamma X$ expressed in terms of the scaling variable $x_\gamma = 2E_\gamma/\sqrt{s}$. Results are presented for two values of the photon scattering angle: a) $\theta_\gamma = 45^0$, and b) $\theta_\gamma = 90^0$. Shown are curves for three center-of-mass energies: $\sqrt{s} = 10, 58$, and 91 GeV.

TABLES

TABLE I. Electroweak V-A coupling constants

| | |
|-------|---|
| v_e | $(-1 + 4 \sin^2 \theta_w) / (2 \sin 2\theta_w)$ |
| a_e | $1 / (2 \sin 2\theta_w)$ |
| v_q | $(I_3^q - 2e_q \sin^2 \theta_w) / (\sin 2\theta_w)$ |
| a_q | $-I_3^q / \sin 2\theta_w$ |

TABLE II. Isospin and fractional charges for quarks

| | I_3^q | e_q |
|---------|---------|-------|
| u, c, t | 1/2 | 2/3 |
| d, s, b | -1/2 | -1/3 |

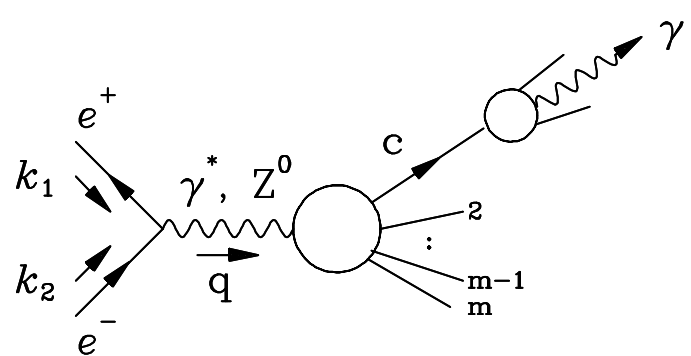


Fig.1

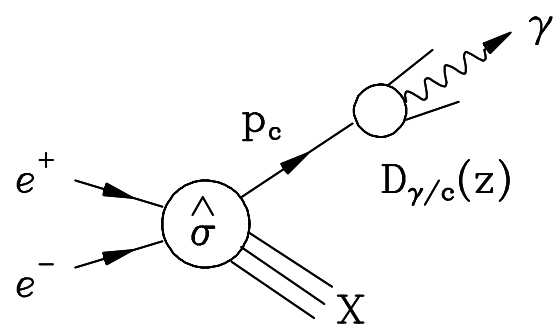


Fig.2

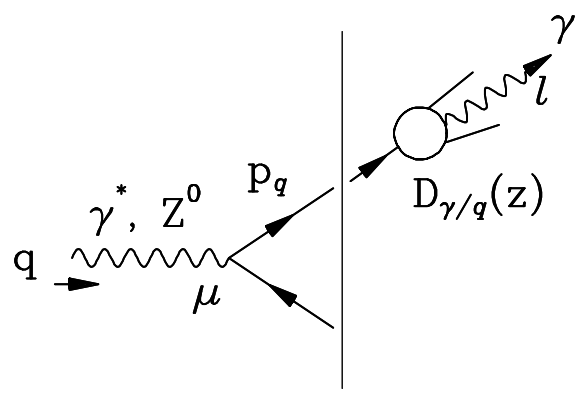


Fig.3

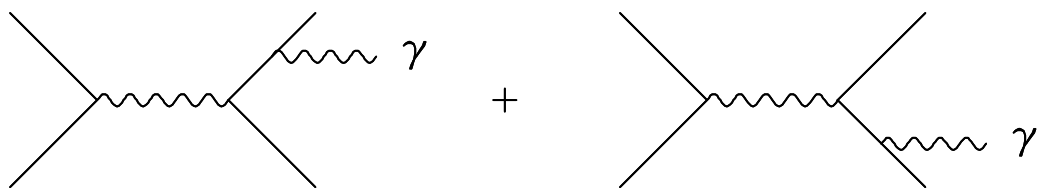
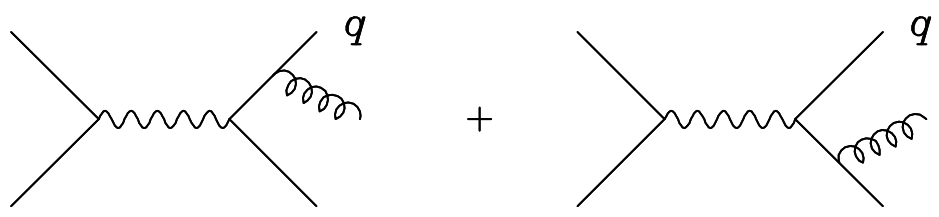


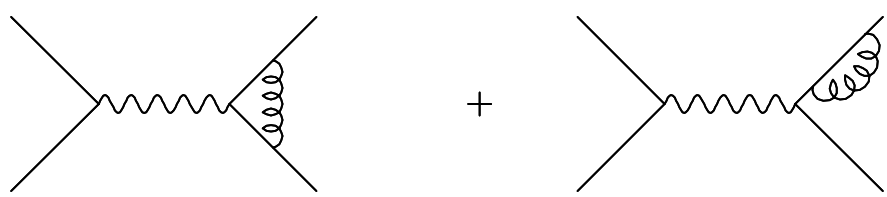
Fig.4



Fig.5



(a)



(b)

Fig.6

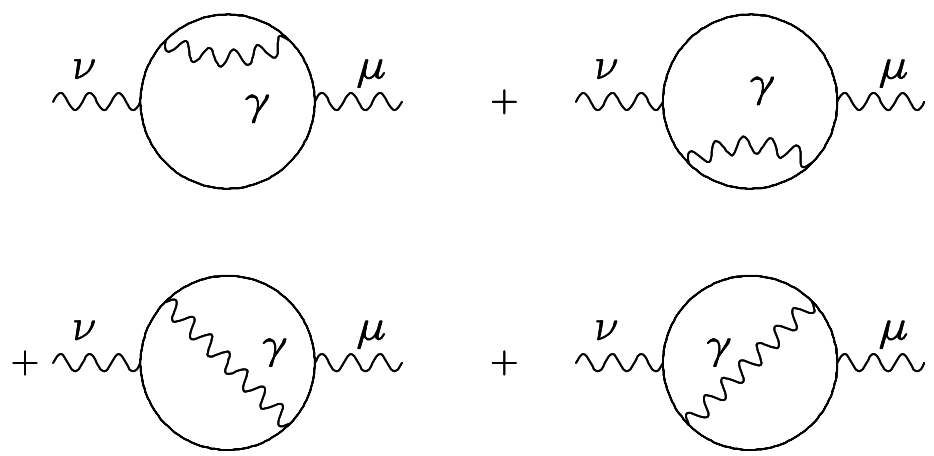


Fig.7

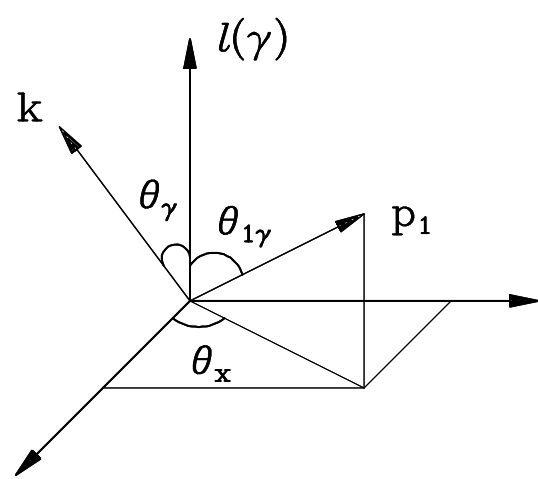


Fig.8

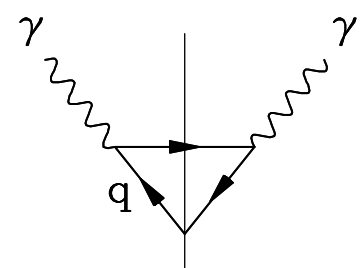


Fig.9

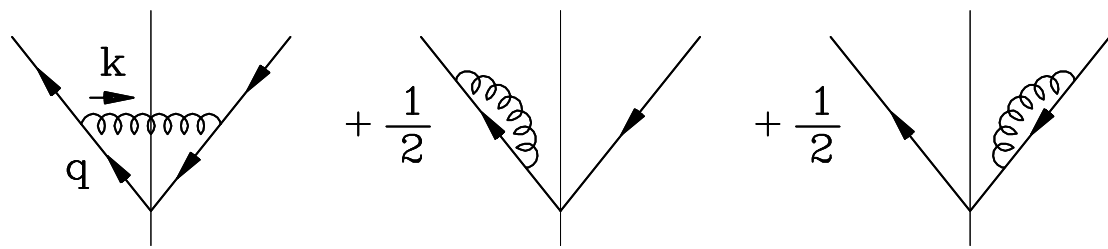


Fig.10

Inclusive Cross Sections

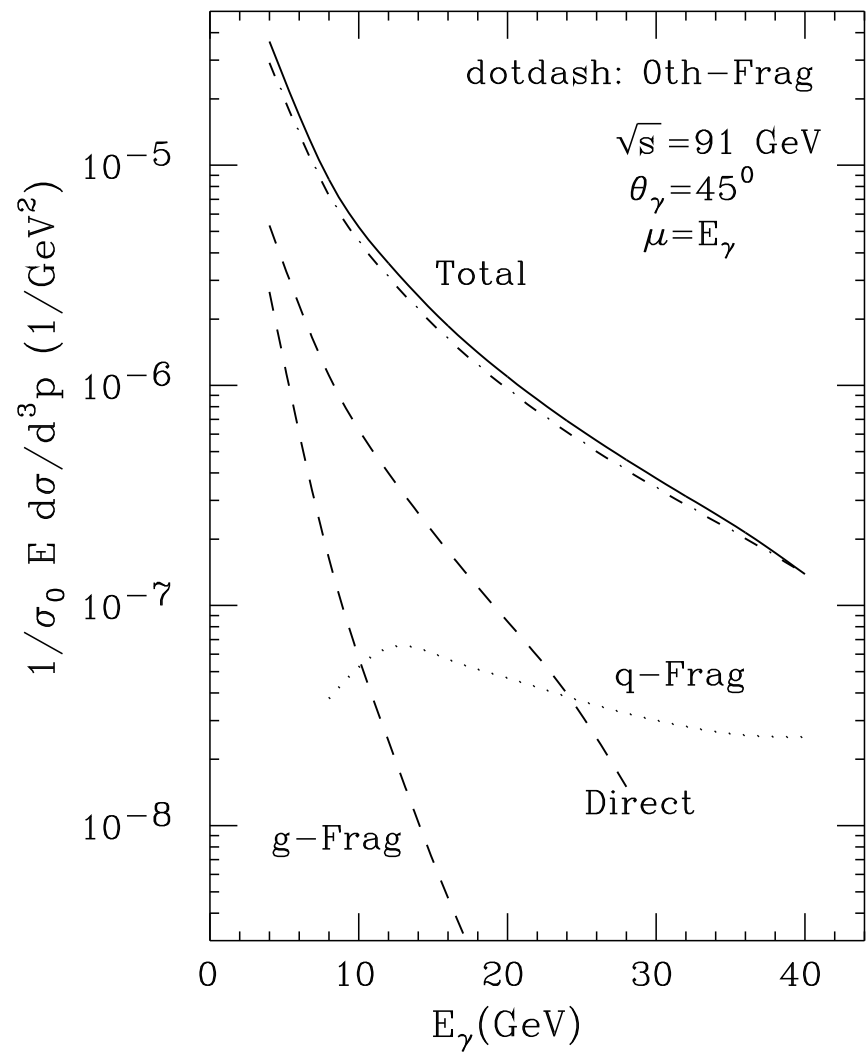


Fig.11-(a)

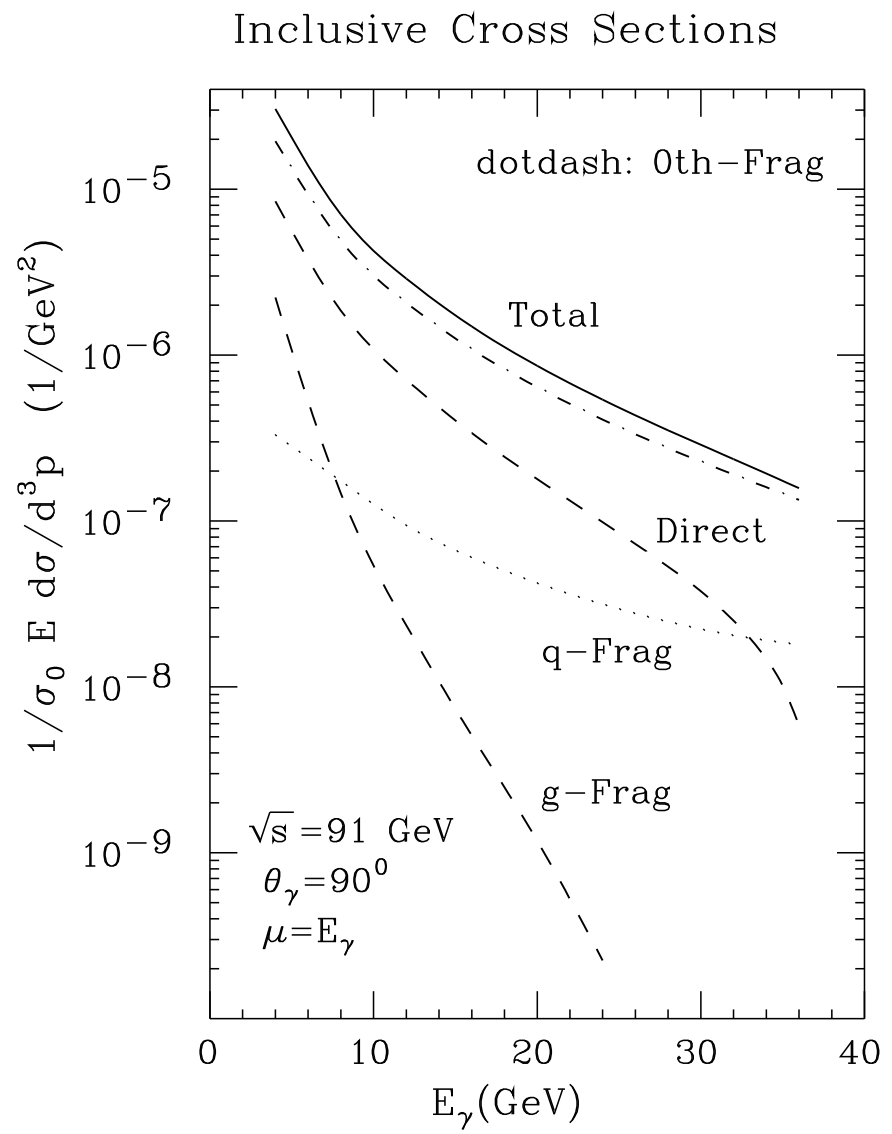


Fig.11-(b)

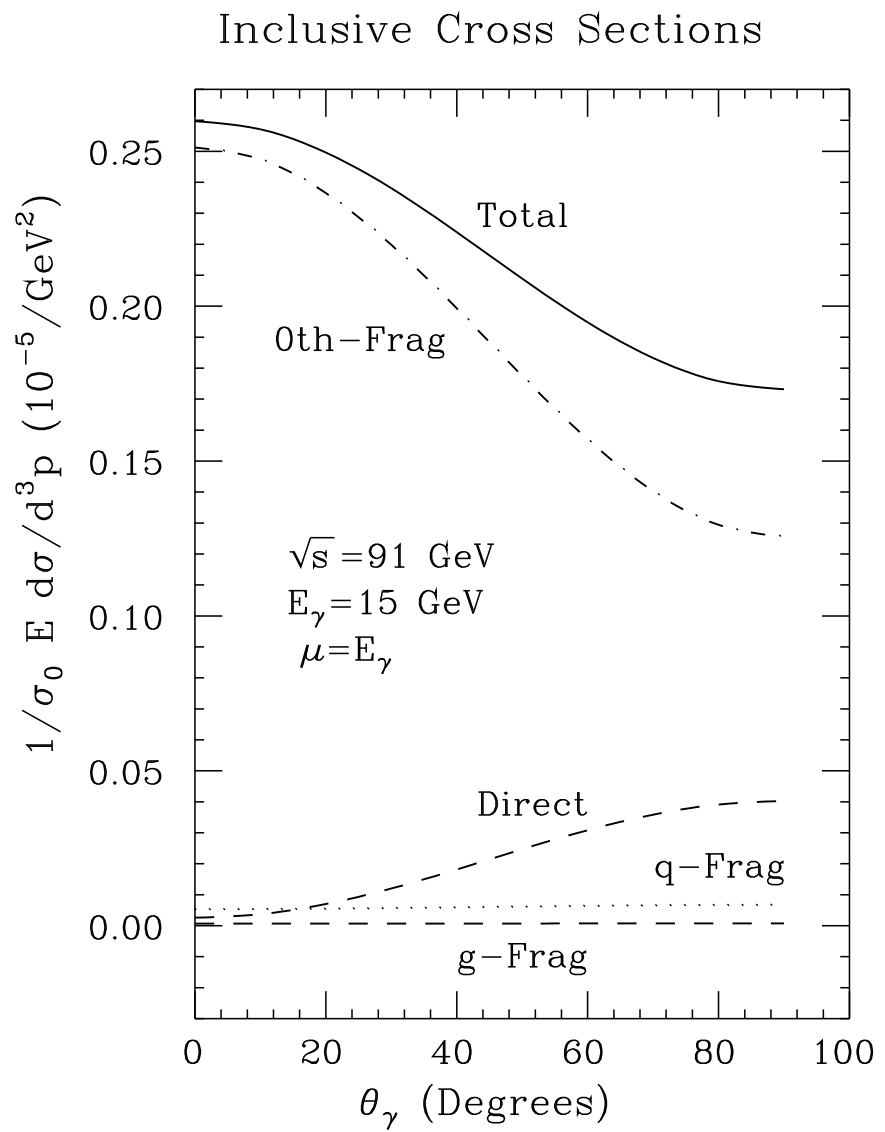


Fig.12-(a)

Inclusive Cross Sections

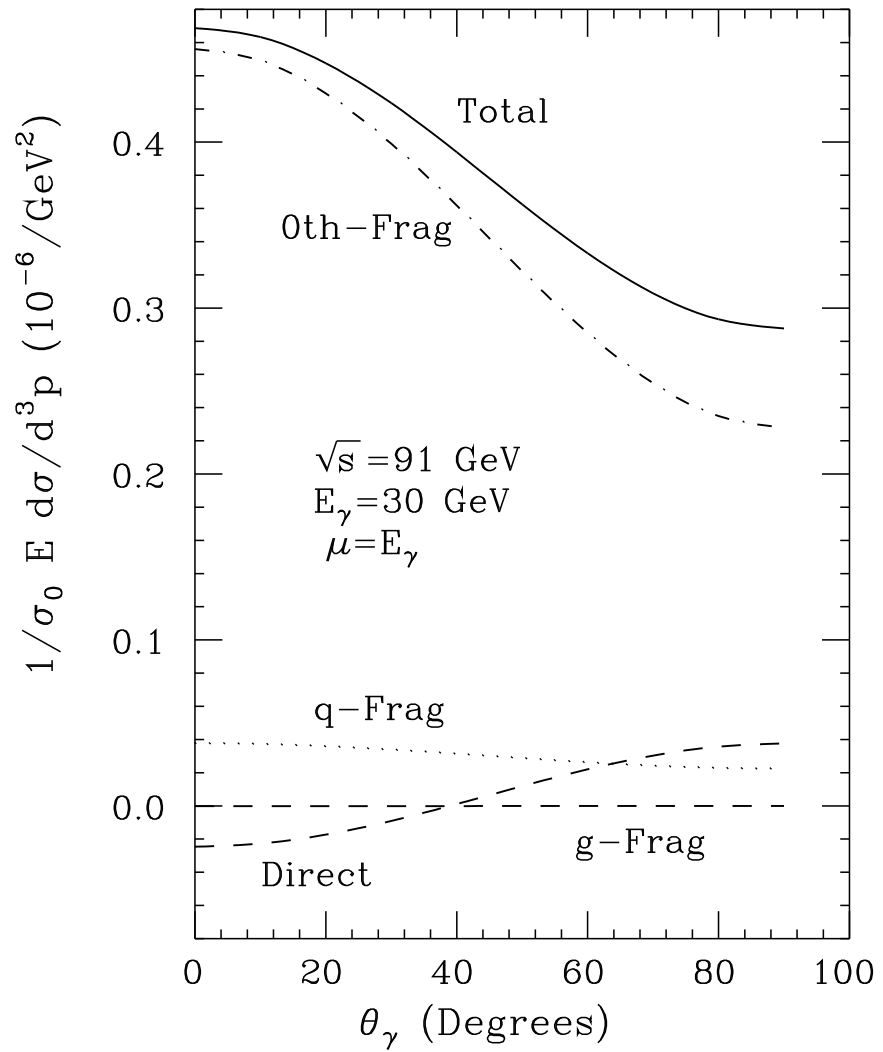


Fig.12-(b)

Inclusive Cross Sections

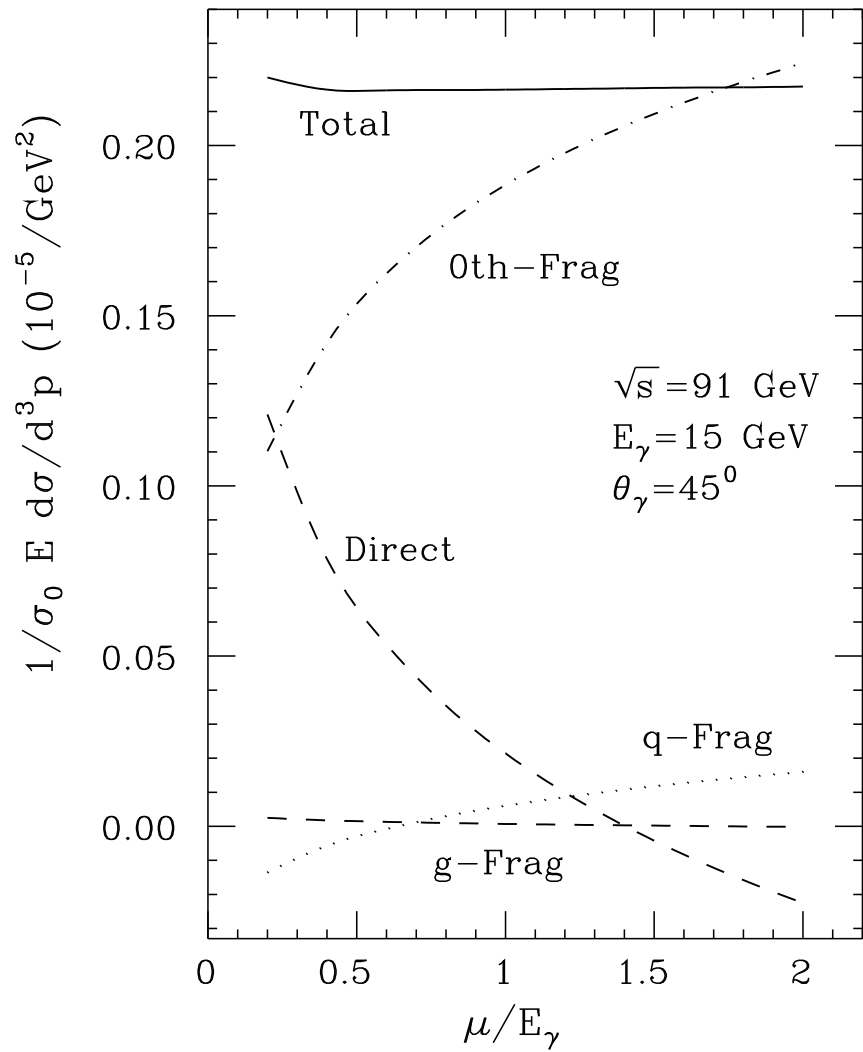


Fig.13-(a)

Inclusive Cross Sections

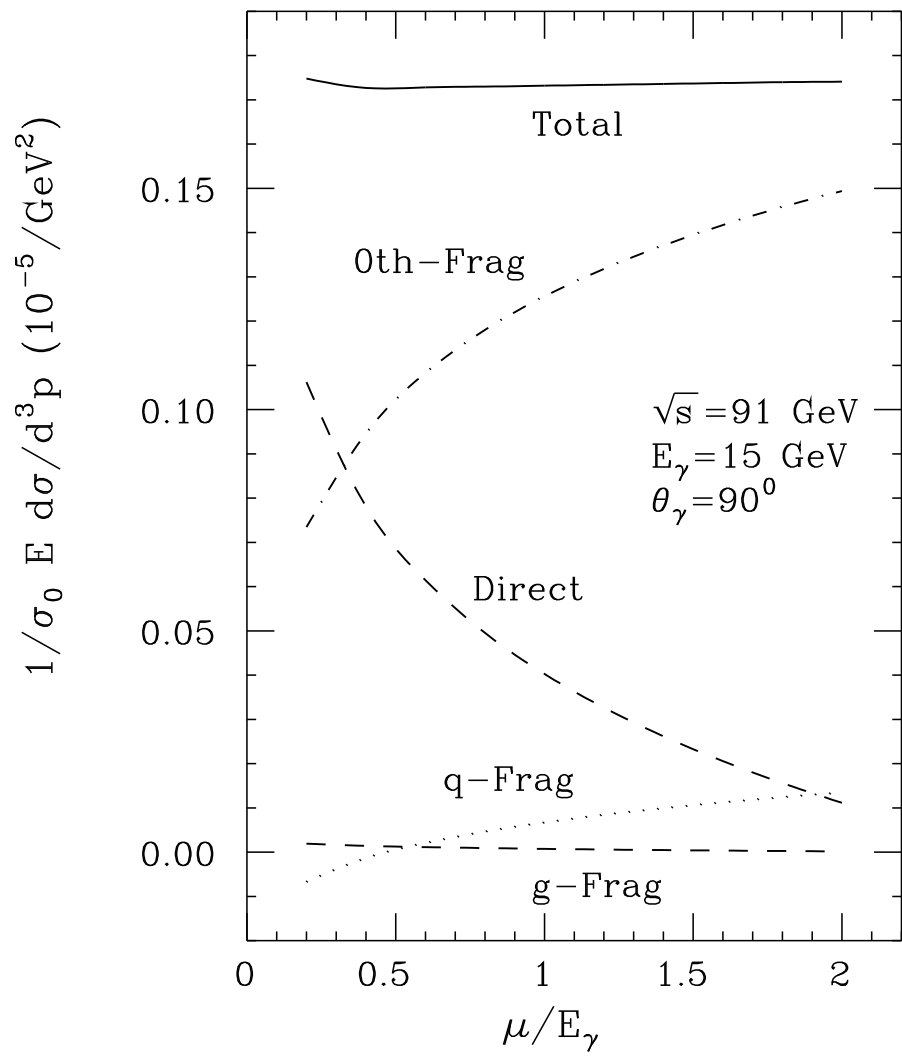


Fig.13-(b)

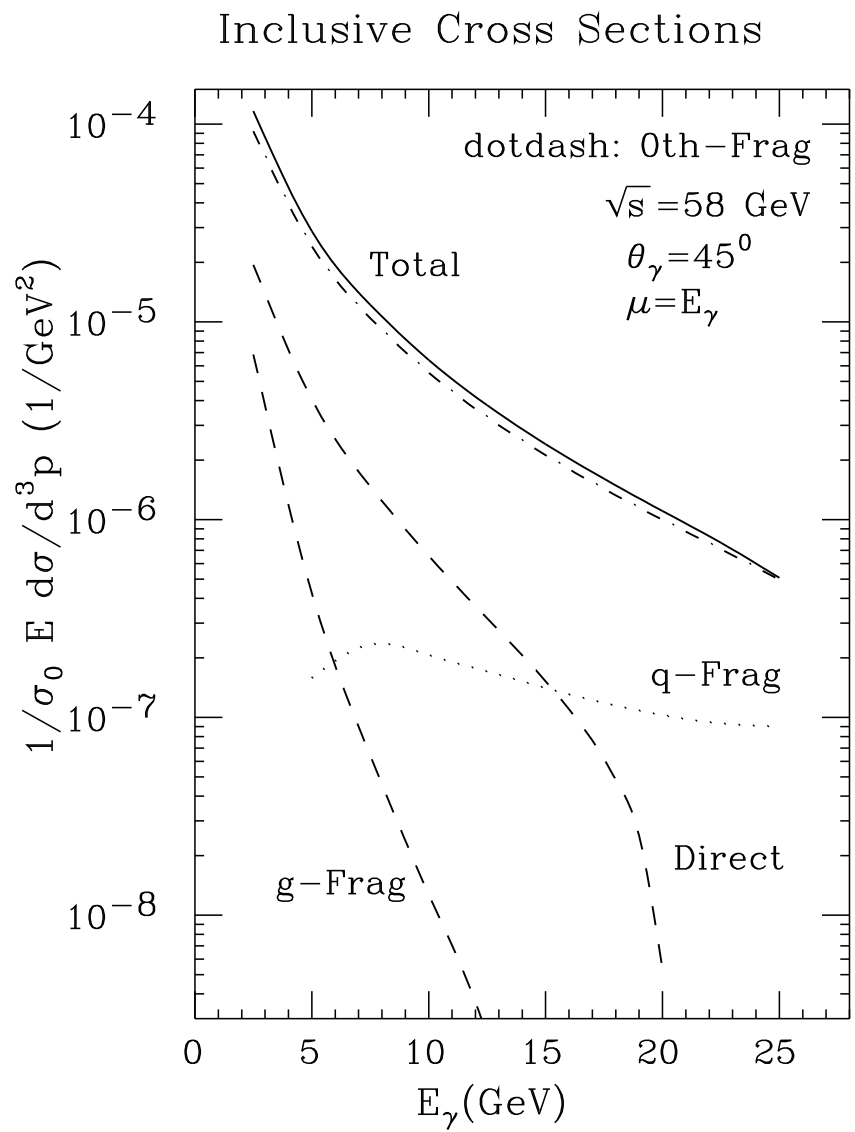


Fig.14-(a)

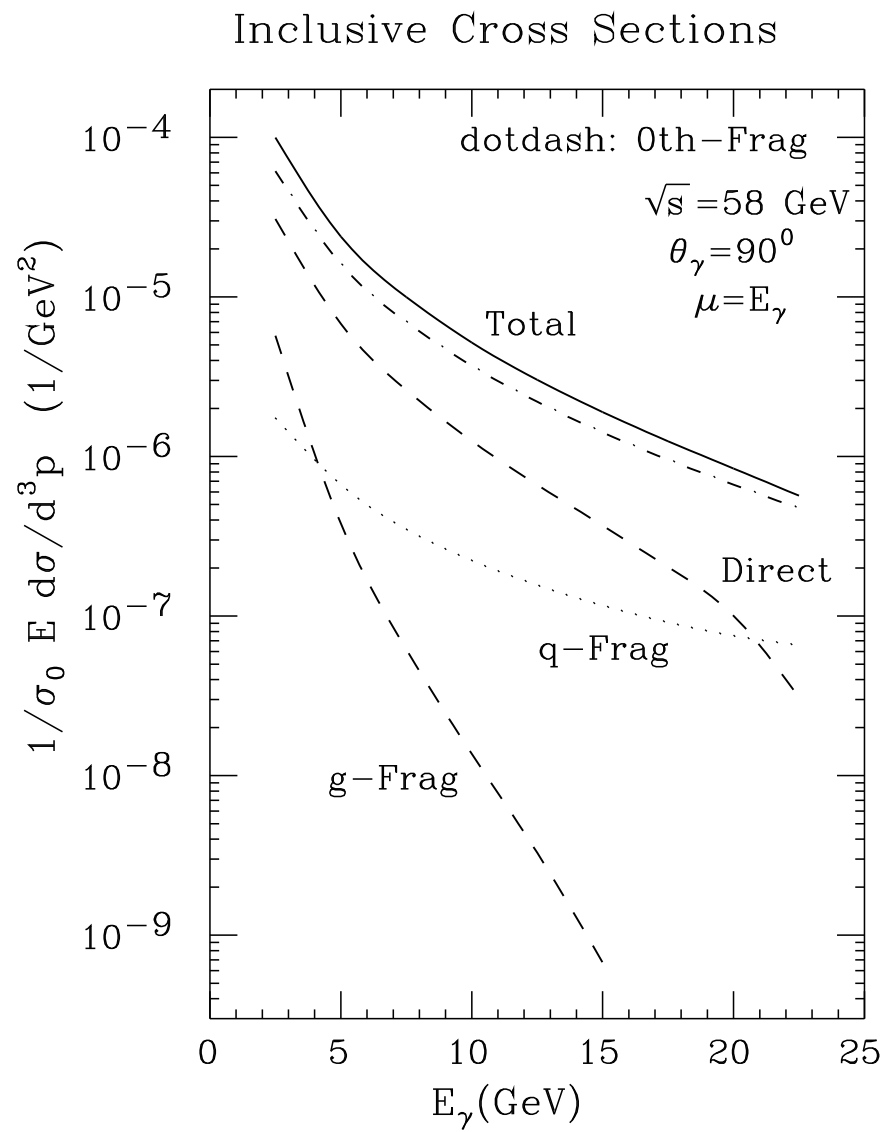


Fig.14-(b)

Inclusive Cross Sections

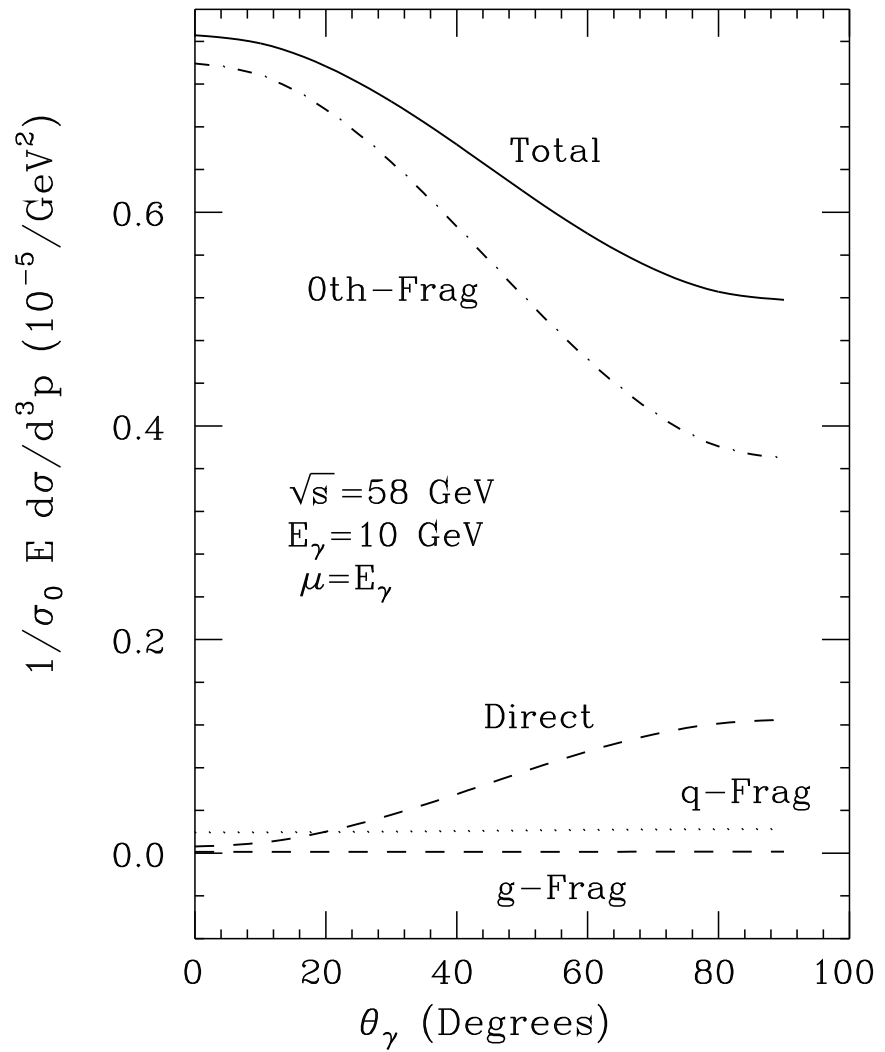


Fig.15-(a)

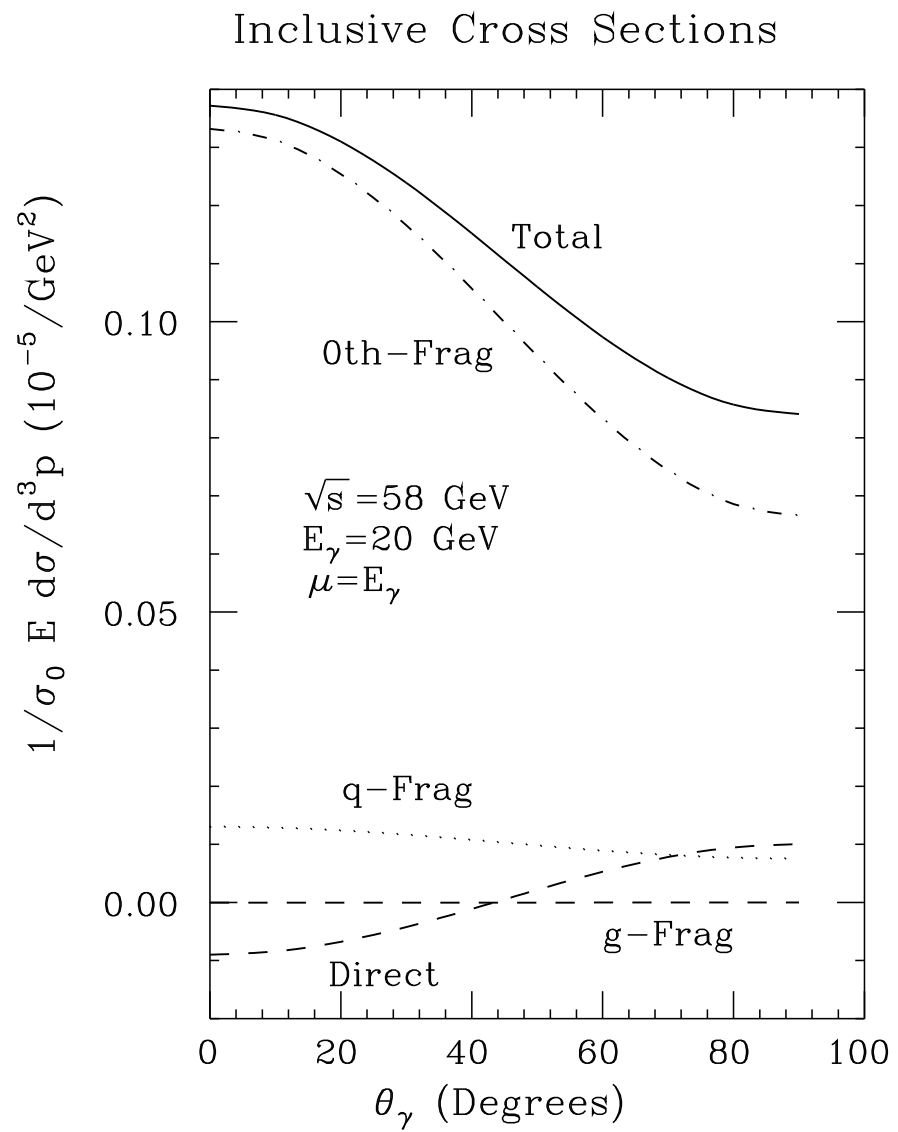


Fig.15-(b)

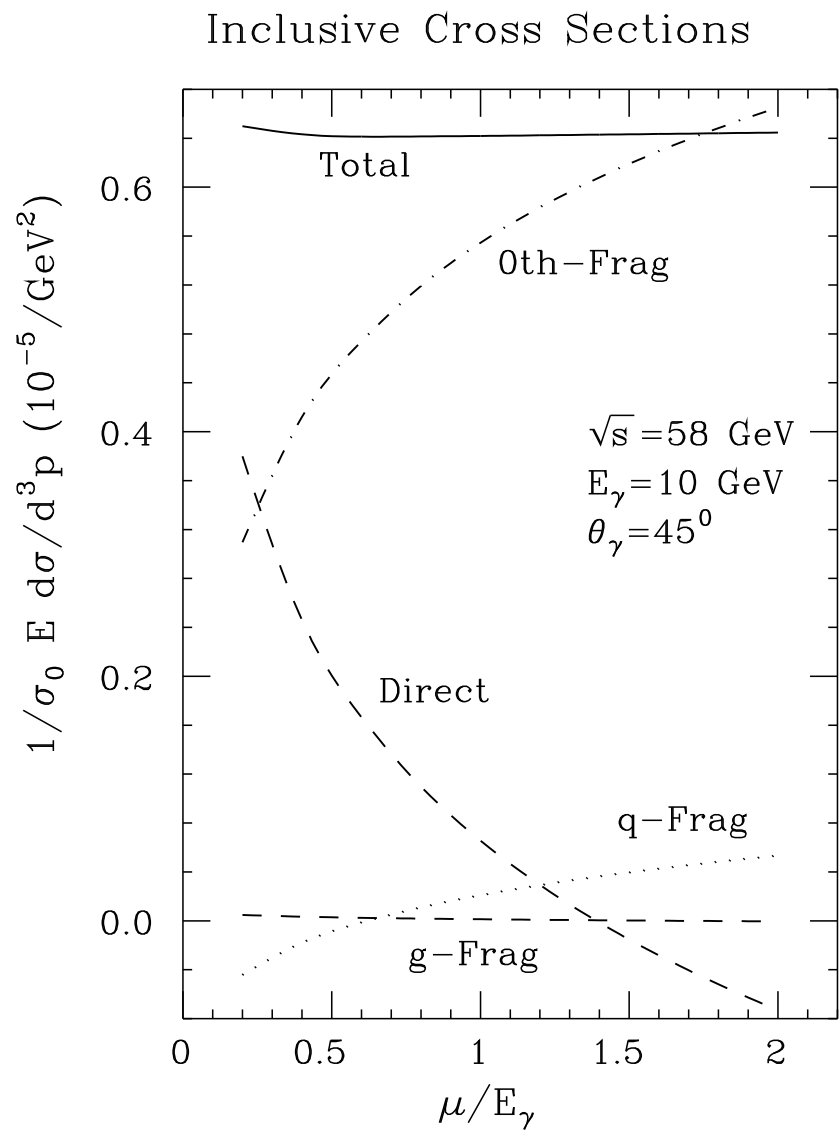


Fig.16-(a)

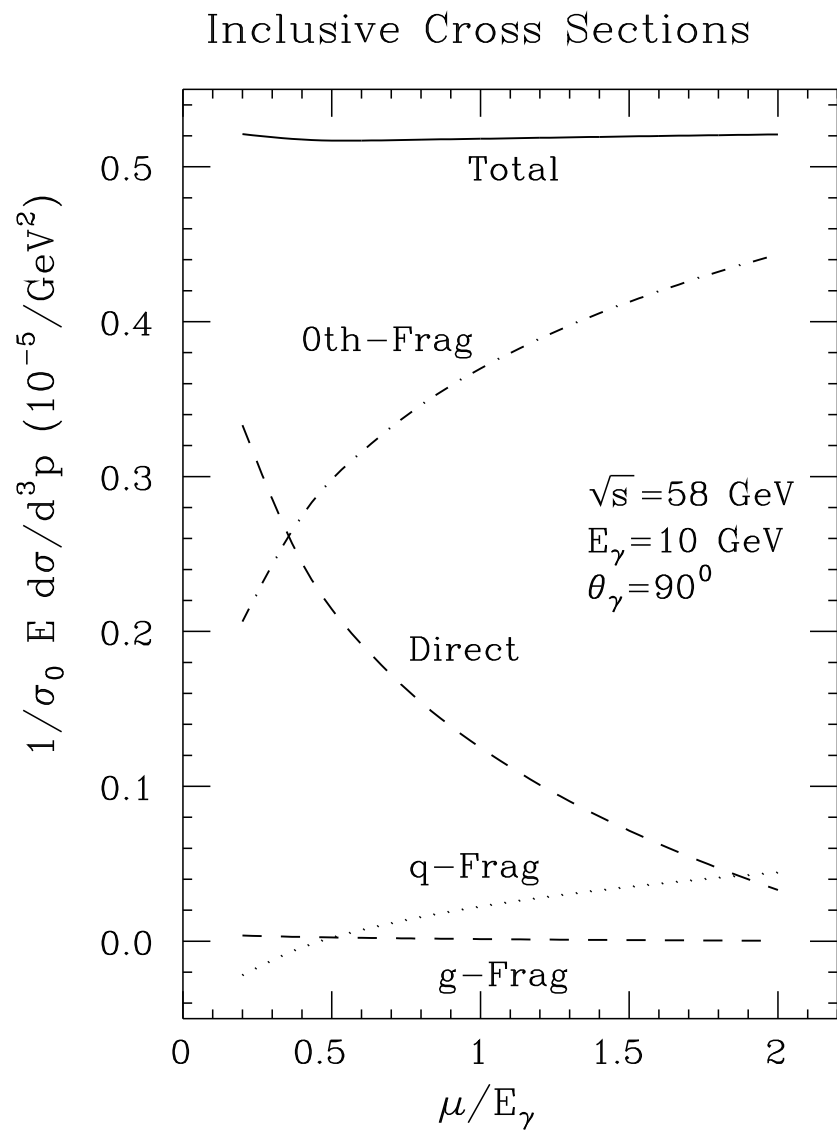


Fig.16-(b)

Inclusive Cross Sections

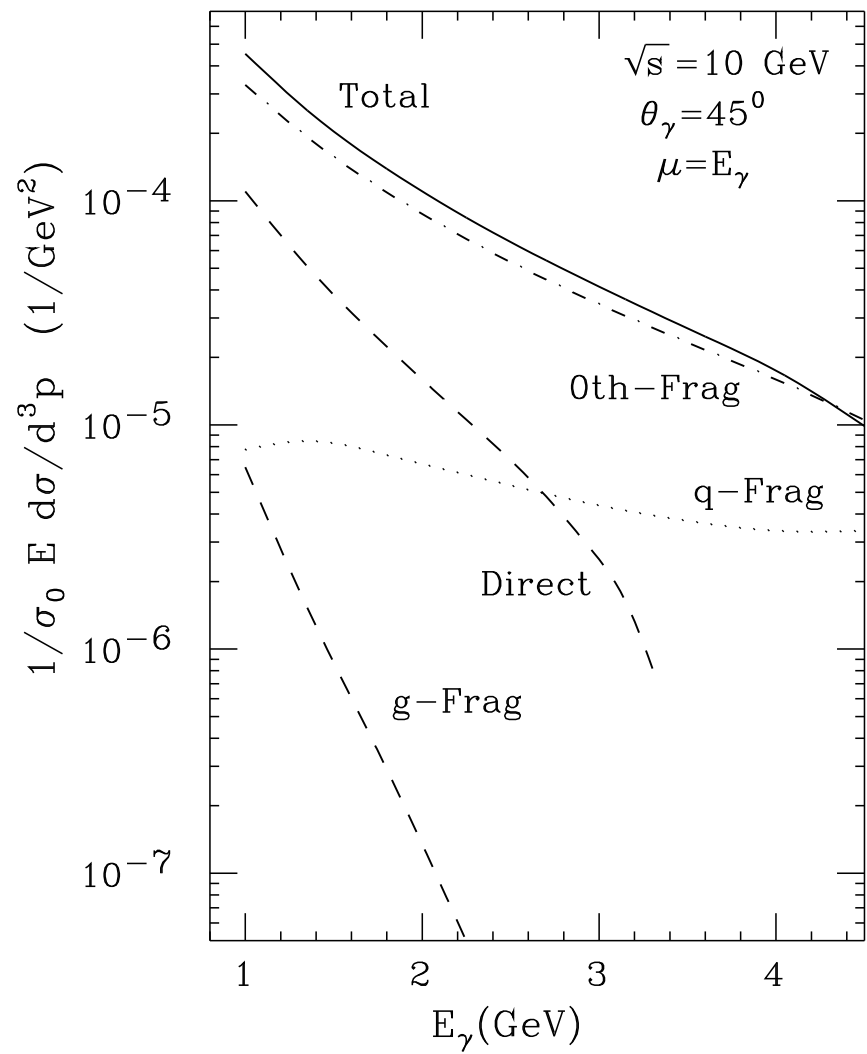


Fig.17-(a)

Inclusive Cross Sections

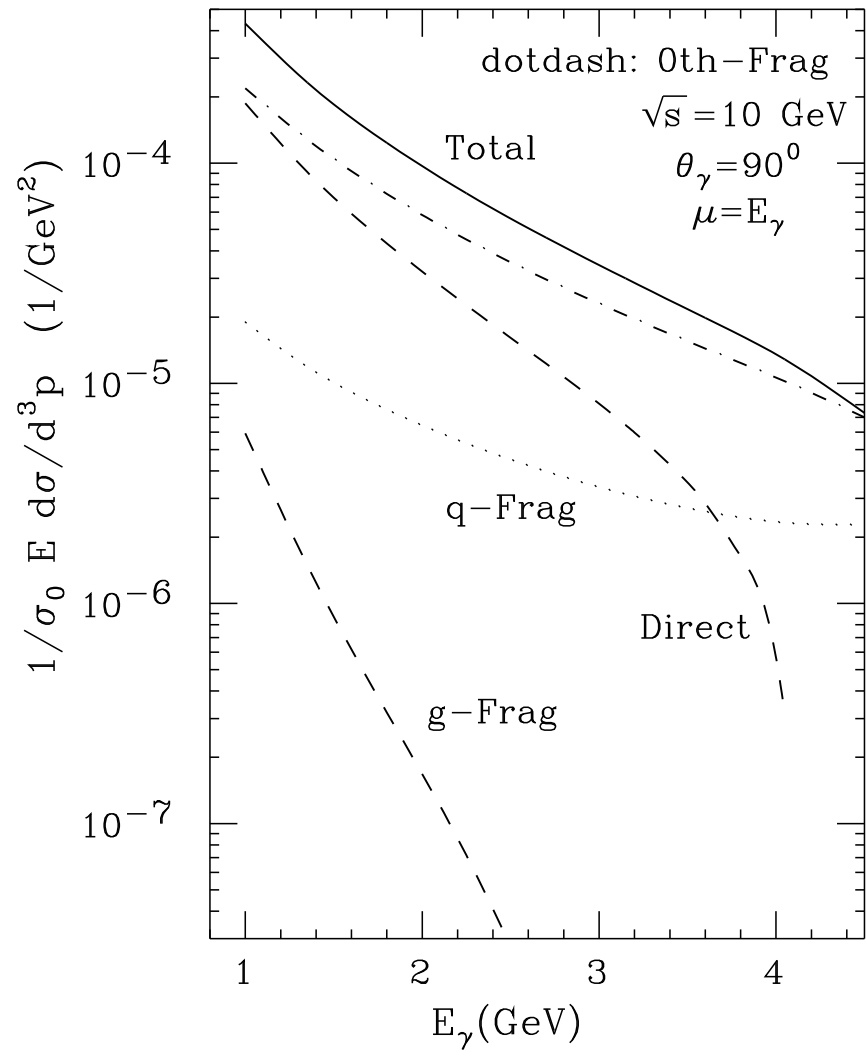


Fig. 17-(b)

Inclusive Cross Sections

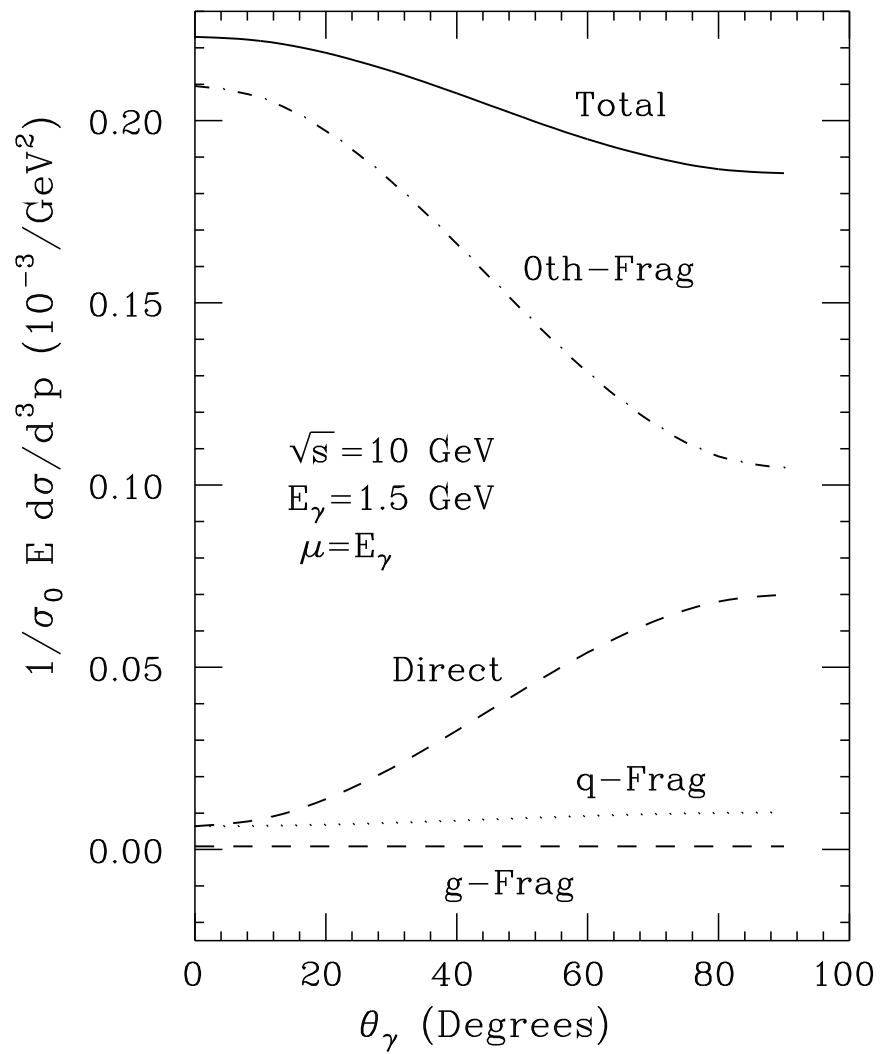


Fig.18-(a)

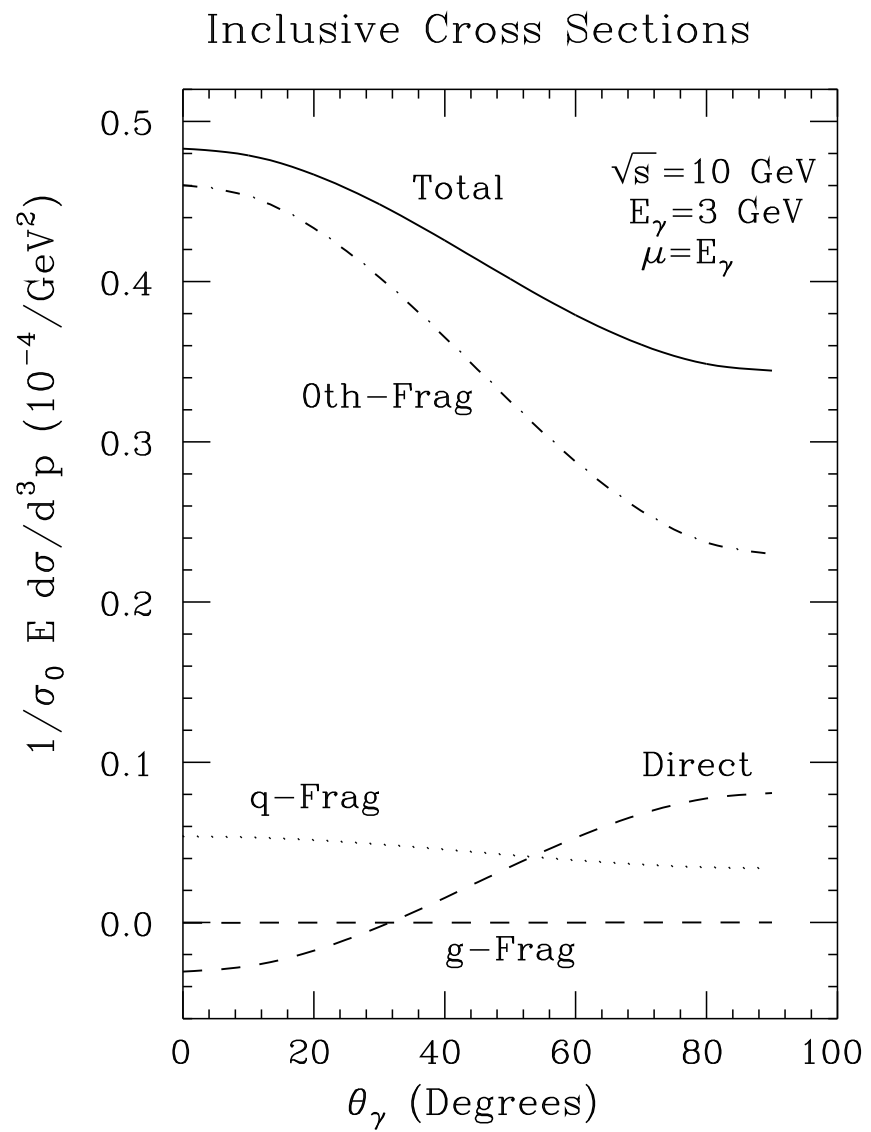


Fig.18-(b)

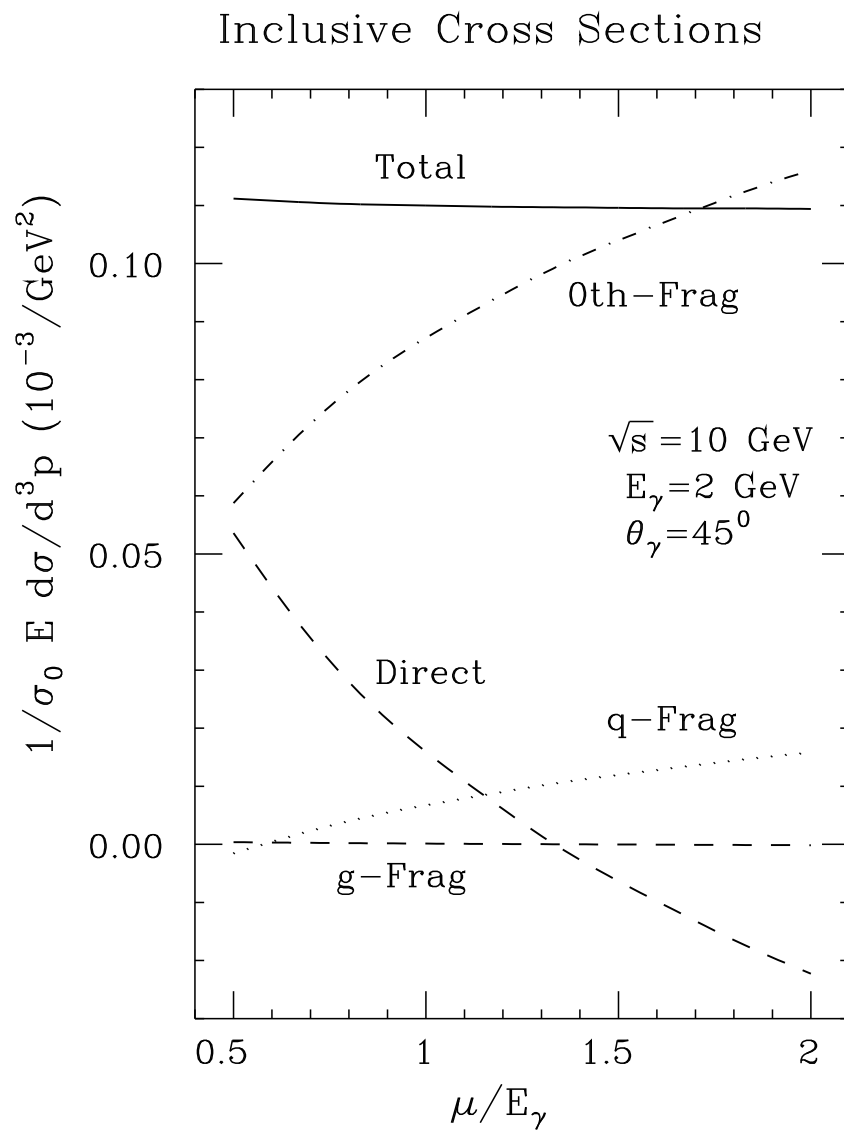


Fig.19-(a)

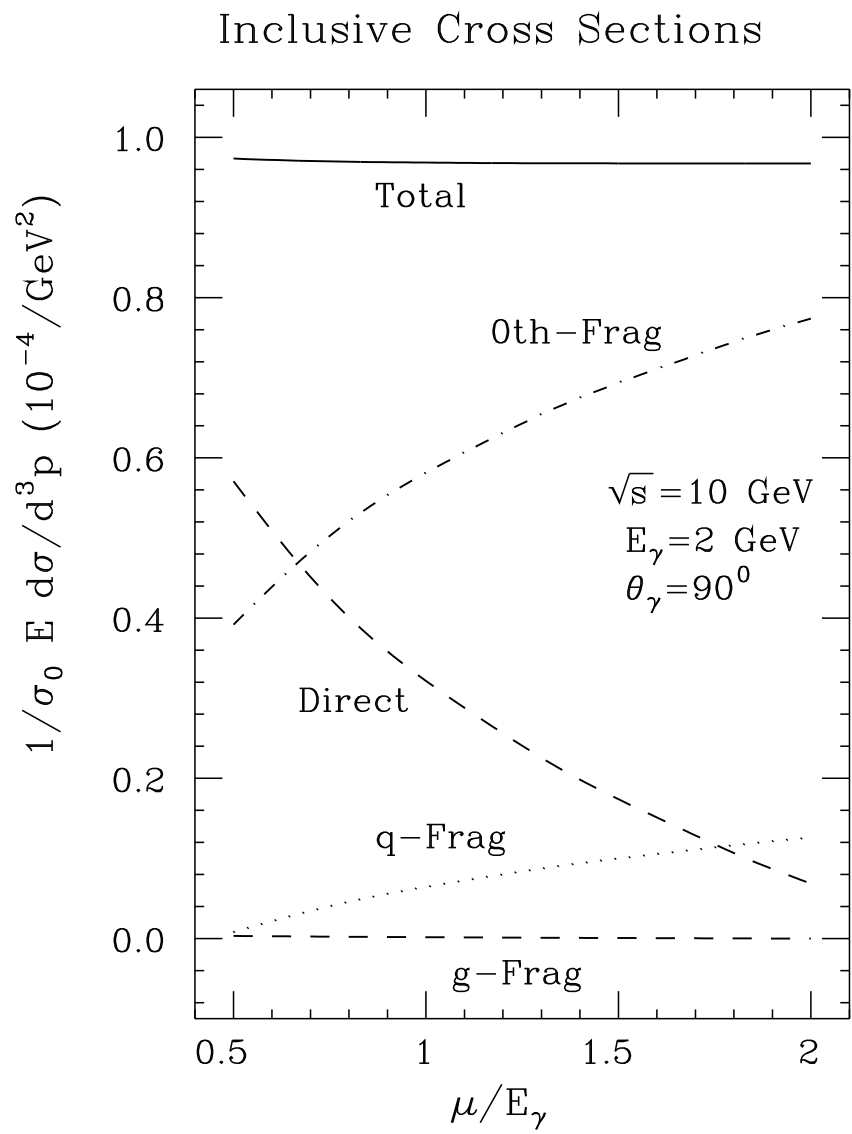


Fig.19-(b)

Inclusive Cross Sections

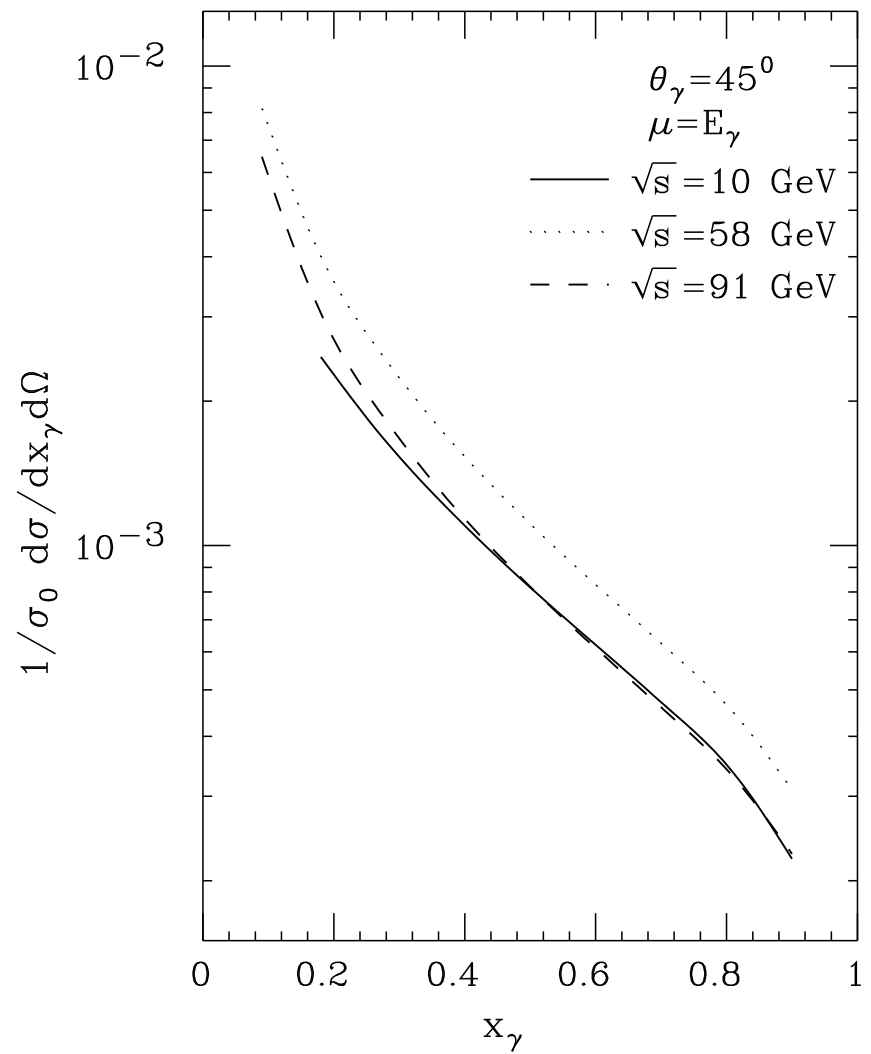


Fig.20-(a)

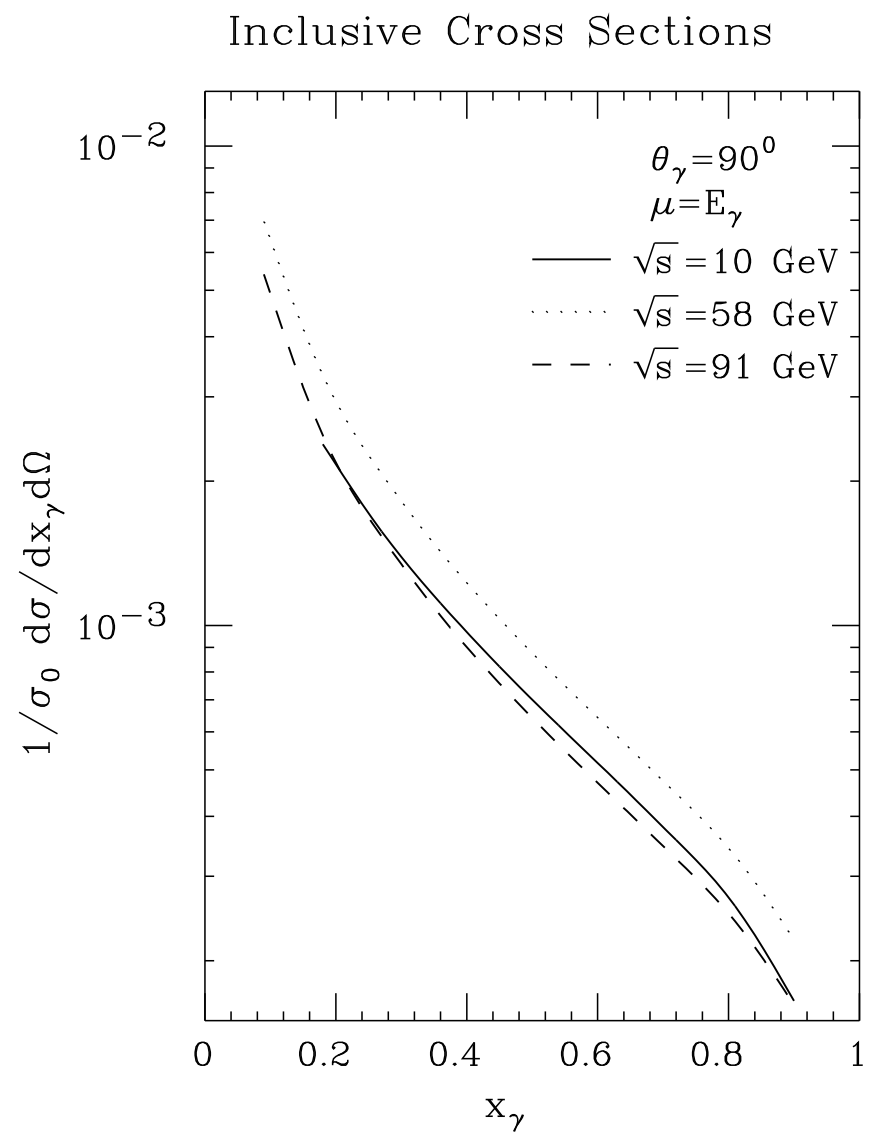


Fig.20-(b)